EVIDENCE FOR PARTIAL EPITHELIAL-TO-MESENCHYMAL TRANSITION (PEMT) AND RECRUITMENT OF MOTILE BLASTODERM EDGE CELLS DURING AVIAN EPIBOLY

A Thesis
Presented to
The Academic Faculty

by

Matthew Futterman

In Partial Fulfillment
of the Requirements for the Degree
Mechanical Engineering in the
School of Mechanical Engineering

Georgia Institute of Technology
January 2011

EVIDENCE FOR PARTIAL EPITHELIAL-TO-MESENCHYMAL TRANSITION (PEMT) AND RECRUITMENT OF MOTILE BLASTODERM EDGE CELLS DURING AVIAN EPIBOLY

Approved by:

Dr. Evan Zamir, Advisor
School of Mechanical Engineering
Georgia Institute of Technology

Dr. Brandon Dixon
School of Mechanical Engineering
Georgia Institute of Technology

Dr. Andres Garcia
School of Mechanical Engineering
Georgia Institute of Technology

Date Approved: [Date Approved by Committee]

ACKNOWLEDGEMENTS

I would like to thank my advisor Dr. Evan Zamir and committee members Dr. Brandon Dixon and Dr. Andres Garcia for their patience, guidance, and support; my labmates: Julia Henkels, Drew Owens, Jaeho Oh, and David Gay for their assistance, support, and friendship; and Dr. Garcia and his lab for training and permitting me to use their confocal microscope.

Lastly, I would like to thank The Woodruff School of Mechanical Engineering, The Parker H. Petit Institute of Bioengineering and Biosciences, and the Georgia Tech community for hosting and supporting myself and my research.

TABLE OF CONTENTS

LIST OF FIGURES AND TABLES

INTRODUCTION

ABSTRACT

Embryonic epiboly has become an important developmental model for studying the mechanisms underlying collective movements of epithelial cells. In the last couple of decades, most studies of epiboly have utilized Xenopus or zebrafish as genetically tractable model organisms, while the avian epiboly model has received virtually no attention. Here, we re-visit epiboly in quail embryos and characterize several molecular markers of epithelial-to-mesenchymal transition (EMT) in the inner zone of the extraembryonic Area Opaca and at the blastoderm edge. Our results show that the intermediate filament vimentin, a widely-used marker of the mesenchymal phenotype, is strongly expressed in the edge cells compared to the cells in the inner zone, and that epiboly is inhibited when embryos are treated with Withaferin-A, a vimentin-targeting drug. Laminin, an extracellular matrix protein that is a major structural and adhesive component of the epiblast basement membrane, is notably absent from the blastoderm edge, and shows three distinct morphological regions approaching the leading edge. While these expression profiles are consistent with a mesenchymal phenotype, several other epithelial markers, including cytokeratin, β-catenin, and E-cadherin, were present in the blastoderm edge cells. Moreover, the results of a BrDU proliferation assay suggest that expansion of the edge cell population is primarily due to recruitment of cells from the inner zone, and not proliferation. Taken together, our data suggest that the edge cells of the avian blastoderm have characteristics of both epithelial and mesenchymal cells, and could serve as an in-vivo model for cancer and wound healing studies.

SIGNIFICANCE

Throughout the second half of the twentieth century and into the new millennium, studies of cell migration have primarily focused on uncovering the mechanisms involved in the motility of individual cells. In the past decade or so, investigators have increasingly turned their attention to the phenomenon of multi-cellular or collective cell migration, since during many developmental and morphogenetic processes, such as gastrulation, neural crest migration, migration of heart primordia, and in several pathophysiologies, notably wound healing and cancer, cells move together in cohesive sheets or continuous streams (Bellairs, Ireland et al. 1981; Bellairs 1986; Bachvarova, Skromne et al. 1998; Davidson, Hoffstrom et al. 2002; Jacinto, Wood et al. 2002; Keller, Davidson et al. 2003; Christiansen and Rajasekaran 2006; Zamir, Rongish et al. 2008). Consequently, newer models, including the posterior lateral line of the zebrafish and dorsal closure in Drosophila (Kiehart, Galbraith et al. 2000; Jacinto, Wood et al. 2002; Ledent 2002; Ghysen and Dambly-Chaudiere 2004), have emerged to address the unique mechanisms that drive and regulate collective cell migration. The most widely studied, and the focus of this study, is the collective cell behavior of a migrating epithelium; for which we used the area opaca (AO) of the developing chick embryo.

Rorth (2009) defines a cell migration phenomenon as collective if the cells move together, making contact at least some of the time, and if they affect one another while migrating. For a sheet to move collectively it must maintain confluence and provide a motive force, else the cells would “tear” the sheet apart and remain stationary. The most widely studied collective cell behavior is the migration of an epithelium, and perhaps, the best known experimental model for epithelial migration is the classic "scratch wound" assay. The biophysical mechanisms involved in epithelial migration are complex (Rorth, 2009), and only recently, using

techniques first developed for studies of individual cells, have some direct measurements of the forces contributed by individual cells within and at the "free edge" of a migrating epithelial monolayer been made in vitro (du Roure, Saez et al. 2005; Farooqui and Fenteany 2005; Trepat, Wasserman et al. 2009). In theory, there are two basic modes of epithelial migration or expansion. On one end of the spectrum, all the cells in the collective migrate cohesively and uniformly, with each cell contributing similar amounts of substrate traction force (du Roure et al., 2005). Alternatively, the cells constituting the free edge could generate the bulk of the traction force necessary for expansion, and thus, "tow" the cells within the interior of the epithelium passively along for the ride (Omelchenko, Vasiliev et al. 2003; Poujade, Grasland-Mongrain et al. 2007), see Figure 1. In the latter case, one can imagine that the interior epithelial cells rest on a basement membrane and are convected by the edge cells, which adhere to and crawl (autonomously) on an extracellular substrate. Clearly, it is important to distinguish between these two general cases, so that any particular model system can be characterized and studied appropriately, and the mechanisms underlying motility better understood.

Developmentally, epiboly, the spreading and migration of the leading edge, is well-studied. It is accomplished with a thin ring of cells at the edge of the blastoderm migrating radially outward across the *in-ovo* deposited (acellular) vitelline membrane, which spreads across it engulfs the entire yolk surface (Figure 2 shows a diagram of a chick embryo). Interestingly, these edge cells are the only cells in the embryo which are attached to this substratum, with the blastoderm resting on a basal lamina of fibronectin and laminin (Critchley, England et al. 1979; Bortier, De Bruyne et al. 1989; Chernoff 1989; Lash, Gosfield et al. 1990; Raddatz, Monnet-Tschudi et al. 1991). Owing to the large size of the egg yolk relative to, for example, *Xenopus* or zebrafish, avian epiboly requires expansion of the AO several hundred-fold over its initial area

(New 1959; Bellairs, Bromham et al. 1967; Downie 1976). *Xenopus* and zebrafish have similar conserved mechanisms of epiboly. The generalized process with both models begins at the animal cap where two distinct layers form: the enveloping layer (EVL), a thin squamous epithelium, and the yolk syncytial layer (YSL), a multinucleated cell. The EVL and YSL expand together with the EVL using the YSL as a substratum until epiboly completes at the vegetal pole (Keller 1980; Trinkhaus 1984; Wood and Timmermans 1988; Fink and Cooper 1996; Zalik, Lewandowski et al. 1999; Ingber 2006).

Other developmental processes involving collective cell migration is the well-studied morphogenetic movement known as dorsal closure in *Drosophila*, and branching morphogenesis as a form of organogenesis. Dorsal closure involves the uniform elongation and progressive advance of two lateral epithelial sheets to displace the underlying amnioserosa and complete the fusion of both sheets (Koppen, Fernandez et al. 2006; Toyama, Peralta et al. 2008); an actin/non-muscle myosin II mechanism is thought to regulate this process. Branching morphogenesis is the process by which sections of an epithelial sheet form simple shapes which are progressively remodeled into increasingly complex structures thereby facilitating the development of organs such as the lungs and kidneys (Friedl 2004; Keller 2005; Ingber 2006; Vasilyev, Liu et al. 2009).

In addition to being paramount in development, collective cell migration also plays an important morphogenetic role with wound healing being a particularly good example. Martin (Martin and Lewis 1992) was the first to show the presence of a filamentous cable of actin around embryonic wounds which was suggested to act as a "purse string" to seal the wound, accompanied with a persistent "smoothing" of the epithelial edge. Similar results were seen by Ihara (Ihara and Motobayashi 1992) in fetal rat skin, Mandato (Mandato and Bement 2001) in Xenopus oocyte wounds, and Brock (Brock, Midwinter et al. 1996) in wounded embryonic chick

wing buds. In these studies, the actin cable only affected the leading edge cells, while the epithelium as close as 2 – 3 cells behind maintained a classic epithelial shape. Figure 3 shows a schematic of an epithelial wound during repair and subsequent cell shape rearrangements and shuffling. Interestingly, even in adult wounds actin cables can still form, though the edge is characterized by the development of filopodia and lamellipodia at the leading edge of the wound which "crawl" to close the wound (Danjo and Gipson 1998; Jacinto, Martinez-Arias et al. 2001), and the healing may or may not be due to contraction of the purse string as in embryos.

The classic epithelial cell is tightly bound to surrounding cells through E-cadherin, whose extracellular site forms adherens junctions, with E-cadherin from adjacent cells, and are coupled to the cytoskeleton through its cytoplasmic tail to β-catenin, which in turn is linked to actin (Jou, Stewart et al. 1995; Kokkinos, Wafai et al. 2007). The presence of cytokeratin is also a hallmark of epithelial cells. Cytokeratin is a member of the intermediate filament (IF) family of proteins, whose name is derived from its physical size which is intermediate between the microfilaments (such as actin) and microtubules, and is believed to regulate mechanical stress (Kolega 1986; Goldman, Khuon et al. 1996; DePianto and Coulombe 2004; Chou, Flitney et al. 2007; Magin, Vijayaraj et al. 2007). In epithelial cells, cytokeratin networks are linked to adjacent cells through desmosomes, the IF analog to adherens junctions (Green and Jones 1996; Gallicano, Kouklis et al. 1998; Green and Gaudry 2000; Garrod, Merritt et al. 2002), and are anchored to the ECM by hemidesmosomes, the IF analog to focal adhesions. See Figure 4 for a schematic of an epithelial cell.

It has been noted that the phenotype of individual cells within an epithelial monolayer in vitro varies widely and is often somewhere in between the dogmatic notions of epithelial and mesenchymal (Revenu and Gilmour, 2009). Whereas cells in the interior of an epithelial

monolayer display prototypical tight junctions, and express the classical epithelial markers, like cytokeratin and E-cadherin, the cells at the free edge may take on a more “mesenchymal-like" phenotype, exhibiting down-regulation of E-cadherin and β-catenin, as well as a flattened morphology and dynamic protrusions of lamellipodia and filopodia (see Figure 5 for a diagram of the collective migration of an epithelium and Figure 6 for other types of cell migration modes). For example, Chaffer reported that different members of the TSUPr1 bladder carcinoma cell line can express both epithelial (E-cadherin and β-catenin) and mesenchymal markers (vimentin and matrix metalloproteases) (Chaffer, Brennan et al. 2006). Klymkowsky and Savagner (2009) refer to this dual nature as the "metastable phenotype", which has also been called "partial EMT" (Arnoux, Nassour et al. 2008; Revenu and Gilmour 2009; Cannito, Novo et al. 2010), see Figure 7.

Previous studies of avian epiboly several decades ago noted a spread morphology and loss of epithelial polarity of the blastoderm edge cells (Downie and Pegrum 1971; Chernoff 1989), prompting us to now investigate the extent to which these cells exhibit a "mesenchymal-like" or pEMT phenotype, using several EMT-informative markers. Our results show, to our knowledge, for the first time, robust co-expression of the mesenchymal marker vimentin and the epithelial markers β-catenin, E-cadherin, and cytokeratin at the free edge of an intact migrating epithelium in an embryonic model system. The results of a BrdU incorporation assay strongly suggest that the cells at the edge of the avian blastoderm are not proliferative, and expansion of the edge cell population is due exclusively to recruitment of cells from the adjacent inner epithelial zone of the AO. These data appear to resolve a decades-old question of how the edge cell population is maintained during avian epiboly (Downie 1976). Finally, using Withaferin A, a small molecule anti-tumor agent recently shown to act through vimentin filaments (Bargagna-

Mohan, Hamza et al. 2007; Bargagna-Mohan, Paranthan et al. 2010), we were able to immediately and completely block epiboly, suggesting that vimentin plays an important functional role in this process.

SPECIFIC AIMS

Specific Aim 1: Characterization of the blastoderm edge using established epithelial and mesenchymal markers.

An advantage of the avian embryo is the preservation of its endogenous substrate, deposited *in ovum* known as the vitelline membrane, during embryonic culturing. **Our hypothesis is that the leading edge expresses both epithelial and mesenchymal traits.** We will characterize epithelial and mesenchymal markers at the leading edge and inner zone (the epithelium between the area pellucida and leading edge with well-defined squamous and cuboidal cells) of Stage 4-5 embryos. Immunoflourescent staining for the extracellular matrix proteins fibronectin and laminin, epithelial markers β-catenin and E-cadherin, mesenchymal markers vimentin and keratin, and rhodamine phalloidin to stain for F-actin will be used to examine the leading edge.

Specific Aim 2: Elucidate the extent to which Rac and vimentin are necessary for edge cell migration.

The small GTPases Rac, Rho, and Cdc42 are known to collectively help in modulating actin polymerization, contraction, and migration. Also, the intermediate filament family of proteins are thought to regulate mechanical stress within cells. **Our hypothesis is that Rac and the IF vimentin are necessary for edge cell migration.** We will test this by using the Rac inhibitor NSC23766 which disrupts actin polymerization and lamellipodia formation, and Withaferin-A, a plant-derived anti-tumor and anti-angiogenesis small molecule that has very recently been shown to antagonize vimentin polymerization.

Specific Aim 3: Determine the contributions of migration and proliferation in maintaining the edge cell population.

During epithelial sheet migration the cells must interact to maintain confluence during expansion or else the sheet would tear**. Our hypothesis is that a combination of cell proliferation and migration acts to recruit new cells to an expanding leading edge.** We will use bromodeoxyuridine (BrdU), a compound used to identify proliferating cells, to track regions of proliferation and migration near the leading epithelial edge.

METHODS AND MATERIALS

METHODS

Fiber Orientation

The ImageJ plug-in, OrientationJ (Fonck, Feigl et al. 2009), was used to calculate the orientations of vimentin filaments. The program uses a Gaussian-shaped window as a weighting function to specify a ROI, then a 2x2 positive-definite "structure tensor" is formed and defined as:

$$J = \langle \nabla f, \nabla f^T \rangle_w = \begin{bmatrix} \langle f_x, f_x \rangle_w & \langle f_x, f_y \rangle_w \\ \langle f_x, f_y \rangle_w & \langle f_y, f_y \rangle_w \end{bmatrix}$$

$$\text{where, } \nabla f = (f_x, f_y)$$

The first eigenvector of the structure tensor gives the dominant direction of the ROI. To compute the orientation distribution of the fibers a structure tensor is formed and evaluated at each pixel in the image. For this study, two Gaussian shaped windows of (σ = 1, σ = 5) were used. The default settings (Minimum Coherency = 70%, Minimum Energy = 10%) were left unchanged. An orientation of 0º indicates a horizontal fiber orientation; orientations of ±90º indicates vertical orientation.

Intensity Profiles

Each image was first converted to 8-bits in ImageJ, adjusting the brightness and contrast for visual clarity, and setting the maximum and minimum intensity values to between 0 and 255 under Plot Profile Options. Line profiles were generated by drawing vertical lines ~256 pixels apart. Row average intensity profiles were generated by tracing the entire image in a rectangle

and selecting vertical profile which row averages, rather than column averages the intensities in the rectangular region.

Cell Counting

The Analyze Particles command was used to trace and count cells, and the Area Fraction measurement option was chosen. Images were prepared by converting to 8-bits and subtracting the background with a rolling ball radius of 100 pixels. To threshold the image, the automatic thresholding command Make Binary command was first attempted. If this did not produce an acceptable image manual thresholding was used. Slight adjustments with the ISSData algorithm tended to produce good results. Next, the Watershed command was used to separate large regions where the thresholding had merged cells together. To properly trace the cells, a minimum cell area was needed below which the program would not outline any particles, otherwise even a 1 pixel dot would be counted as a cell. For these images a pixel area between ~20 to ~50 pixels was sufficient. Lastly, selecting the Show option under Analyze Particles provided a drawing of the traced cells to compare against the original image.

BrdU Staining

Lyophilized BrdU was added to EC culture media to a final concentration of 10μM. Making BrdU aliquots is not advisable since BrdU does not store well in solubilized form, and fresh solubilized BrdU was added for each experiment. Embryos were exposed to the BrdU + EC culture media for 20 minutes at 37ºC (a *pulse*). Then, the embryos were transferred to standard (untreated) EC culture media for 4 hours at room temperature (a *chase*). 0 hour embryos were fixed at this stage according to protocol, and 8 hour embryos on standard EC culture media were returned to the 37ºC incubator for 8 hours (*incubation*). Following the incubation period, these embryos were fixed and stained according to protocol as well.

An order of magnitude higher concentration was also tried (100 μM), though other than increased immunoflourescent intensity in the higher concentration, the samples did not appear to differ in general structure and form. It should be noted that previous BrdU protocols (Sanders, Varedi et al. 1993; Hammerle and Tejedor 2002) indicated that concentrations as low as 10 μg/mL to as high as 5 mg/mL yielded positive stains as well in the chick embryo, though these were in liquid media and *in-ovo*, respectively.

Fixation and Mounting

Embryos were fixed in 3% paraformaldehyde (PFA) for 30-60 minutes at 4°C, and permeablized for 45 minutes using 0.5 or 1% Triton X-100 also at 4°C. Ice cold methanol (100%) was added for 30 minutes. A series of ethanol solutions of 90%, 70%, 50%, 30%, and 15% were applied for 15 minutes each to rehydrate specimens. We would like to note that in routine whole mount immunofluorescence studies in chick embryos, either detergent or methanol are used alone for the permeabilization step. In our hands, we found that using these solutions in combination resulted in embryos that were much cleaner and more free of lipid yolk droplets, resulting in better imaging, especially at the thin blastoderm edge. Furthermore, using methanol as the primary permeabilization step often resulted in loss of preservation of the blastoderm edge, which was obviously critical for this study. Blocking buffer (3% BSA in PBS) was applied from 8 hours to overnight, followed by application of primary antibodies overnight, a second round of blocking for at least 4 hours, and finally secondary antibodies were applied overnight in blocking buffer. Subsequently, to label nuclei, embryos were incubated in a solution containing

Sytox Green (500 nM in PBS) for 15 minutes. All incubation steps were carried out on a gentle rocker, which greatly improved immunofluorescence by minimizing yolk particles. It should be noted that previous studies have suggested that cytokeratin is particularly susceptible to loss of antigenicity upon PFA fixation (Klymkowsky et al., 1987); however, we found that by using relatively brief PFA application (30 minutes) at 4°C, immunofluorescence labeling was preserved. For actin filament labeling, rhodaminephalloidin (Cytoskeleton Inc.) was diluted 1:1000 from 14 μM stock and applied for 4 hours.

To mount embyros for confocal microscopy, excess PBS and yolk was absorbed gently using a Kimwipe and the embryos were placed ventral side down on a glass slide. The paper ring surrounding the embryo was carefully cut away, leaving the blastoderm attached to the vitelline membrane. This step has to be done very carefully to avoid excessive wrinkling of the vitelline membrane and folding of the blastoderm edge onto the AO. Any remaining fluid was again absorbed, and approximately 20 μL of Prolong Gold antifade reagent with DAPI (Invitrogen, Carlsbad, CA) was gently applied to the embryo, followed by an 18 mm cover slip. After remaining covered at room temperature overnight, clear nail polish was placed around the edges of the cover slip. This procedure ensured very flat specimens, without having to use xylenes or clearing agents.

Microscopy

A Nikon C1 confocal microscope system was used for all immunofluorescence imaging. Nikon 20x Plan Apo (dry) or Nikon 60x Plan Apo (oil) were used exclusively. Time-lapse images taken with a Leica DM6000B microscope, and a Leica 2.5x objective.

Image Processing

ImageJ (and necessary plug-ins) and Photoshop were used to construct and analyze the images.

MATERIALS

Antibodies

Vimentin (H5), laminin (3H11), fibronectin (B3/D6), and cytokeratin (1h5) monoclonal antibodies were obtained from the Developmental Studies Hybridoma Bank (The University of Iowa); polyclonal anti-β-catenin (ab6302) was obtained from Abcam (Cambridge, MA); monoclonal anti-E-cadherin (36/E) was obtained from BD Transduction Labs (Franklin Lakes, NJ); Sytox Green dead cell stain was obtained from Invitrogen (Carlsbad, CA). Secondary antibodies were purchased from Jackson ImmunoResearch Labs (West Grove, PA) and ThermoFisher Scientific (Waltham, MA). All antibodies were diluted to a concentration of 1 μg/mL. Sytox Green was used at a concentration of 500 nM in whole mounts, and 1 μM during time lapse imaging.

Pharmaceuticals

A 10-mM stock solution of Withaferin A (Tocris Bioscience) was aliquoted and frozen at -20°C. Embryos were incubated on Withaferin A-treated agar-albumen culture media plates (50 μM) or DMSO control plates for 4-8 hours.

Quail Embryos

Japanese quail (*coturnix coturnix*) eggs were purchased from the Ozark Egg Company (Stover, MO) and incubated for 2.5 hours in a humidified chamber at 37°C. The embryos were cultured using a modified New culture technique (Chapman, Collignon et al. 2001) with 9/16" filter paper rings on semi-solid agar/albumen media, and incubated overnight for a total incubation time of approximately 24 hours until embryos reached Hamburger-Hamilton (HH) stage 4-5 (Hamburger and Hamilton 1951).

RESULTS

SPECIFIC AIM 1: CHARACTERIZATION OF THE BLASTODERM EDGE

Nuclei Patterns

The edge cell region is easily distinguished from the cells in the interior by its much lower cell density (Fig. 8C), and thus, all immunofluorescence images are accompanied by nuclear labeling to establish the edge zone region for each marker. The primary area of interest in this study was the outer most region of the AO, including the blastoderm edge cells (Fig. 8A-C). It is important to note that the size or width of the edge cell region varies from a few nuclei (Fig. 8I) to over a dozen between different embryos (Fig. 8G). It has been suggested in previous studies that the edge zone size may be developmentally regulated (Bellairs, Bromham et al. 1967; Downie 1976), but we observed a significant amount of variation of edge zone size even for embryos of approximately similar stages.

Intermediate Filaments (Cytokeratin and Vimentin)

Vimentin was found to be strongly expressed at the blastoderm edge (Fig. 8D, 11A), and much more weakly, yet still positive, throughout the interior region of the AO (Fig. 8D, 11B). In general, an abrupt transition was observed between the interior and edge zones. The edge cells displayed a dense interconnected filamentous network and bright clusters or foci, which often appear to be "cupped" around one side of the nuclei (Fig 11A). We also observed individual or bundled vimentin filaments in the edge cells. Though not measured these filaments appeared to extend several microns, sometimes tens of microns, which is significantly larger than the reported persistence length of ~1 um (Mucke, Kreplak et al. 2004), suggesting that vimentin filaments in the edge cells bear significant mechanical loading (tension). In contrast to the edge

zone, vimentin expression within the interior of the AO consisted mostly of tortuous "squiggles" or "whirls", and a higher cell density (Fig. 11B). Moreover, we did not observe dense vimentin clusters adjacent to the nuclei in the inner zone.

By examining the orientation of the edge cell fibers it was found that for a Gaussian window of $\sigma = 1$ (Fig 9), a normal-like histogram was measured and centered around 0º indicating a horizontal directional preference for VM fibers with an image resolution of 1024x1024 pixels; a vertical orientation is registered as ±90º. However, upon "smoothing" the data with a Gaussian window of $\sigma = 5$, three regions were distinctly preferred and centered around -50º, -25º to +25º, and +50º. Lower resolution (512x512 pixels) orientation measurements were also taken but for both Gaussian windows no distinct orientation was observed, but showed a "dispersed" or random distribution. Fiber orientation measurements within the inner zones showed a randomized distribution at $\sigma = 1$ for both resolutions, and an "apparent" preference for ±50º at $\sigma = 5$ (Fig 10). As noted though, upon a visual inspection the inner zone fibers don't seem to have a preferred direction. Above a Gaussian window of $\sigma = 5$, the data was completely filtered measuring no fibers nor orientations for both the edge and inner zones.

The cytokeratins have been suggested to serve a function in maintenance of epithelial integrity (Magin, Vijayaraj et al. 2007). We observed strikingly different expression patterns compared to vimentin. Most importantly, in contrast to the obvious greater expression of vimentin in edge cells, we did not observe significant differences in cytokeratin levels between the edge zone and interior cells of the AO. In the edge cells, cytokeratin exhibits a "web-like" filamentous network with no apparent perinuclear localization (Fig 8F, 9D). Within the inner region of the AO, cytokeratin filaments appeared form dense networks (Fig 9E, 9F). A similar observation has been made for keratin networks which generally display a pan-cytoplasmic

distribution extending from the nucleus to the cell periphery, making contact at sites of cellular adhesion (DePianto and Coulombe 2004).

Adherin Junction Proteins (β-catenin and E-cadherin)

As expected from previous studies (Roeser, Stein et al. 1999), both β-catenin and E-cadherin expression are restricted to well-defined cell borders within the epiblast cells of the inner region of the AO (Fig 8H, 8J). At the blastoderm edge, E-cadherin and β-catenin are also clearly localized to cell-cell junctions, but appear to be absent from the "free edge" where a cell has no adjacent neighboring cell (Fig 12A,B). We did not observe nuclear β-catenin localization; however, we cannot rule out that there is some cytoplasmic or plasma membrane distribution for both β-catenin and E-cadherin not associated with cell junctions. This mechanism could also explain the observed front-back polarized expression of E-cadherin and β-catenin and apparent cytoplasmic diffusion of both markers if β-catenin is not necessarily being degraded as described in the Wnt pathway nor localized to the nucleus (Huber, Stewart et al. 2001; Christofori 2003) since the edge cells are neither completely epithelial nor completely mesenchymal.

Extracellular Matrix (Laminin)

We observed three distinct regions of laminin immunofluorescence in the AO, the edge zone (EZ), transition zone (TZ), and inner zone (IZ). At the edge, the laminin expression appears punctate, as the basal lamina is broken down. In the "transition zone" (TZ) just behind the edge, long tightly packed individual laminin fibrils originating from the basal lamina are apparent (Fig 13B). Sufficiently far away from the blastoderm edge, the laminin appears as a virtually continuous sheet (Fig. 13C). This sheet-like appearance becomes gradually more ragged and consists of numerous gaps or holes closer to the blastoderm edge. No laminin was observed beyond the leading edge on the vitelline membrane., In all regions we observed nuclei in

between gaps and holes in the basal lamina, indicating that the tissues were intact, and our observations were not simply artifacts of fixation or embryo processing.

Line profiles quantifying the level of immunoflourescent intensity were taken for each region. Each profile was thresholded at an intensity of 50 bits since below this level the gaps in the laminin sheet were observed. The profiles of the EZ (Fig 14) show gaps as small as a few microns to nearly 100 μm wide, and separated by narrow high intensity sometimes saturated regions which supports our punctate EZ observation. The TZ profiles (Fig 15) still show gaps, though the size and number of gaps have decreased compared to the EZ. Interestingly, the IZ profiles (Fig 16) still show gaps in the visually observed matte sheet with intensities more evenly distributed across the region compared to the TZ. Comparing the row average intensity profiles of each region (Fig 17) showed that the TZ and IZ have average intensities of 55.1 ± 16.1 bits and 55.9 ± 16.0 bits, suggesting that both regions have similar amounts of laminin. The EZ has an average intensity of 21.1 ± 6.8 bits, more than half the amount of the TZ and IZ.

SPECIFIC AIM 2: PHARMACEUTICAL INHIBITION

The vimentin antagonizer, Withaferin-A (Lahat, Zhu et al. 2010), was used to disrupt vimentin expression at the leading edge. Time-lapse images showed no discernible expansion, but instead contraction of the AP for embryos treated with 50 μM Withaferin-A (Figure 18), while the marginal zone (MZ), a transition between the AP and AO, appeared unaffected by the treatment. The controls underwent normal epibolic and AP development as indicated with a noticeably larger blastoderm and convergence-extension of the embryo.

Sytox, a DNA-labeling reagent, was added to the media for the entire duration of the experiment at a final concentration of 1μM, to monitor whether epiboly was blocked due to abnormal cell death. Sytox Green becomes fluorescent when the nuclear membrane becomes permeable, thereby allowing the compound to bind to the DNA in the nucleus. Somewhat to our surprise, WFA treatment caused abnormally high levels of Sytox Green incorporation within the AP. However, we did not observe higher incorporation levels, compared to controls, anywhere in the AO or at the blastoderm edge. Since the chosen concentration of Withaferin-A completely stopped epiboly no other concentrations were used. We did not expect the pharmaceutical to have such an immediate and powerful effect, and recovery assays did not restore normal epibolic and AP development.

Subsequent fixation and immunofluorescence showed “prickly” actin protrusions at the leading edge characterized by many filopodia and lamellipodia. Vimentin filaments appear to become collapsed around the nucleus (Fig. 20F), and the cells at the free edge of the blastoderm develop long, spiky filopodial-like extensions (Fig. 20G) that are not seen in control embryos (Fig 20D). Furthermore, this effect only affects the edge zone. WFA and control VM and F-actin

staining (Fig 21) show similar morphologies of the inner zones for both treatments, with similar VM squiggles (Fig. 11B) in the inner zones and cuboidal epithelial cells shown by F-actin.

In addition to treating with Withaferin-A, the Rac1 inhibitor NSC23766 was used to disrupt actin polymerization. Time lapse images were performed at concentrations of 100 μM and 200 μM, then epibolic area measurements were taken using ImageJ by tracing the edge of the blastoderm, and calculating the area (Fig 22). The controls expanded at a normalized rate of ~0.13 mm^2/hr, and although inhibition with a 100 μM concentration showed delayed expansion, the embryos recovered about 10 hours post-treatment reaching a normalized expansion rate of ~0.12 mm^2/hr. However, inhibition with a 200 μM concentration completely nullified expansion. The normalized expansion rate of this higher concentration was ~0.26 mm^2/hr; the doubled value is likely due to embryonic variation. In both cases, the AP continued to develop normally even though AO expansion was slowed or prevented.

SPECIFIC AIM 3: CELL PROLIFERATION AT THE LEADING EDGE

BrdU (bromodeoxyuridine), a synthetic nucleotide which replaces a thymidine group during S-phase, showed labeled cells in the edge zone at 8 hours of incubation post-chase, but no cells immediately post-chase (Fig 23). This observation suggests that some of the cells migrated from the inner zones to the edge zone during the 8 hour incubation period. Computation of the area fractions of BrdU and Sytox labeled cells during each time are shown in Table 1; pre and post-processed images outlining cells to compute the area fractions are shown in Figure 24. The area fraction difference between Sytox and BrdU cells is 7.34% for the 0 hour samples and 8.175% for the 8 hour samples. Assuming the Sytox labeled all the cells, an increase in the number of edge cells by an area fraction of 0.84% represents the percentage of cells Sytox positive and BrdU negative. These cells are most likely to lie within the edge zone since more Sytox positive cells are seen in the edge than BrdU labeled cells in the same region (Fig 23 C, D).

To determine whether these results were statistically significant, a 1-tail t-test with unequal variances was performed on the BrdU and Sytox samples for the 0 hour incubation post-chase, and 8-hour incubation post-chase groups. The research hypothesis, for both stains, states that 8 hours of incubation post-chase increases the area fraction; the null hypothesis states the length of incubation time post-chase does not affect the area fraction. The calculated p-value of BrdU was 0.056 and 0.22 for Sytox thereby rejecting the research hypothesis for both cases. Although, the area fraction of the edge cells appears to increase during the post-chase incubation, the statistics show that this result is likely due to chance. However, the sample sizes for both groups was unequal (n = 5 for 0 hours, n = 4 for 8 hours) and the cell counting algorithm was

optimized for each image thereby increasing Type II errors. Furthermore, only one post-chase incubation time was analyzed; longer post-chase incubation times could yield different results.

In addition to comparing BrdU area fractions, live cell imaging at the leading edge was attempted to determine how cells are recruited to the expanding edge using Vybrant CM DiI cell labeling solution, CellTracker Red CMTPX, and Syto 17 red fluorescent nucleic acid stain from Invitrogen (Carlsbad, CA). However, each of these labels was either negative or inconclusive.

DISCUSSION

The major result of this study is the surprising and novel finding that the intermediate filament vimentin --- a classical marker of the mesenchymal phenotype (Gilles, Polette et al. 1999; Ackland, Newgreen et al. 2003; Kokkinos, Wafai et al. 2007) --- is robustly expressed in the edge cells of the chick blastoderm during epiboly (the rapid expansion of the extraembryonic epithelium). We believe the vimentin expression pattern may be unique to the avian embryo, since a similar expression pattern was not reported for Xenopus (Dent, Polson et al. 1989; Herrmann, Fouquet et al. 1989) or zebrafish (Cerda, Conrad et al. 1998) epiboly in previous immunofluorescence studies. We did not find any reports of in situ hybridization studies for vimentin in Xenopus or zebrafish. Previous vimentin studies in chick did not report blastoderm edge expression (Erickson, Tucker et al. 1987; Page 1989). Our results also show that E-cadherin, β-catenin, and cytokeratin are co-expressed along with vimentin in edge cells; however, the epiblast basal lamina, as shown by laminin immunofluorescence, was clearly broken down in the edge cell region. Taken together, these data suggest that the edge cells of the avian extraembryonic AO employ vimentin in a functional manner, and perhaps, that loss of basal lamina contact causes up-regulation of vimentin expression or polymerization specifically at the blastoderm edge. Furthermore, we hypothesize that vimentin, an IF found in mesenchymal cells and thought to structure the cytoplasm to resist external stresses (Fuchs and Cleveland 1998; Wang and Stamenovic 2002; Guzman, Jeney et al. 2006), is important for promoting rapid migration of the blastoderm edge and spreading of AO during epiboly. Cytokeratins are thought of as the main intermediate filament type expressed in epithelial cells. However, vimentin has been shown to be up-regulated in several epithelial wound healing models in vitro. Furthermore, models of epiboly are relevant to studies of wound healing (New 1959; Chernoff 1989; Weliky

and Oster 1990). Using MCF10A cells in a human mammary epithelium wound healing model, Gilles (Gilles, Polette et al. 1999) showed that vimentin is up-regulated in cells located proximal to or at the free edge, which were involved in active migration towards the center of a lesion. Also, using the same cell line, Pollette et al. (Polette, Mestdagt et al. 2007) showed that in addition to vimentin up-regulation, beta-catenin and ZO-1 display cytosplasmic and/or nuclear localization at the leading edge. Dulbecco (Dulbecco, Allen et al. 1983) reported that NIH 3T3 cells that were cultured, wounded, and stained with the vimentin anti-sera T11A9e show asymmetric migration into the wound, with the forward part of the cell (in the direction of movement) more brightly stained. He suggested that staining is related to cell movement by examining cell colonies where the cells in the dense center did not stain, whereas the highly motile edge was stained brilliantly. Our measurements of the preferential directions of the vimentin filaments towards a normal orientation to the leading edge, and the results of the aforementioned studies, lends credence to our hypothesis of vimentin promoting rapid migration of the blastoderm edge.

If the EZ is indeed highly motile then long EZ vimentin filament lengths also suggests that the EZ is a region of high stress. This is due to the observation of many filaments significantly exceeding the persistence length of vimentin, which is a measure of its flexibility and can be related to Young's Modulus (Mucke, Kreplak et al. 2004). The expansion of the area opaca may be stretching the filaments, which could be acting as "shock" or "stress" absorbers (Janmey, Shah et al. 1998; Herrmann, Bar et al. 2007). This is analogous to straightening a rope by pulling on both ends. Alternatively, the spreading EZ could be causing the squiggles to anneal "end-to-end" or add onto existing long vimentin filaments, a method of filament extension reviewed by Chou and Flitney (Chou, Flitney et al. 2007). The co-expression of some of the

classic epithelial markers (β-catenin, E-cadherin, and cytokeratin), see Figure 12 for further traits, with vimentin in the edge cells is another novel finding of this study. It suggests another form of the "metastable phenotype" in the leading edge, perhaps unique to avian epiboly. Klymkowsky (1982) noted that vimentin and keratin networks are interconnected as shown by injecting monoclonal antibodies against one or the other of these filament systems into PtK2 cells and observing degradation against the other network We believe that the "free edge" induces a mesenchymal-like morphological change in vimentin at the leading edge enabling migration. This is supported by the surprising result of the Withaferin-A (WFA) treatments halting blastoderm expansion, Figure 18, without apparent vimentin degradation. In fact, the vimentin bundles suggest reorganization, rather than inhibition of the intermediate filament. Goldman found a similar vimentin network change with microinjections of the vimentin 1A peptide which caused the network to shift from a fully spread configuration to a rounded morphology (Goldman, Khuon et al. 1996). The morphology change of branching to ‘filamentous aggregates’, is also similar to the phenotype generated by soluble tetrameric vimentin (vimentin ‘particles’) in *in-vitro* filament polymerization assays treated with WFA (Bargagna-Mohan, Hamza et al. 2007), though our observed aggregates are at a “macro” cellular level compared with the perinuclear region, respectively. A possible cause of these ‘macro’ aggregates is the inability of VM to maintain stability in the presence of the suggested large tensile forces present in the edge, since WFA is degrading or at least partially inhibiting long filamentous VM formation. Any sufficiently long VM filaments would simply “collapse” from the strain. Furthermore, these aggregates or “collapsed filaments” are likely directly inhibiting the normally motile, spreading edge cells, which have a “branched” filamentous form. A possible reason for the non-motility lies in the fact that vimentin (in particle, ‘squiggle’, or long filament

form), unlike other IF's rapidly reorganizes within cells through bi-directional movement along the microtubule network (Gyoeva and Gelfand 1991; Prahlad, Yoon et al. 1998; Yoon, Yoon et al. 2001; Clarke and Allan 2002), which could cause VM to travel coherently along microtubule tracks.

Furthermore, the fact that epiboly was blocked completely and immediately after the start of treatment, and since Sytox incorporation was restricted to the AP, the effects of the drug are likely not due to transcriptional changes, but rather directly to effects on the cytoskeleton and motility of the edge cells. Indeed, recent studies have shown that WFA suppresses human breast and prostate cancer cells' growth *in-vitro* and *in-vivo* by inducing marked apoptosis (Srinivasan, Ranga et al. 2007; Yang, Shi et al. 2007; Lahat, Zhu et al. 2010). And, several lines of evidence suggest that WFA has anti-cancer properties, manifested by directly targeting tumor cells and indirectly impeding tumor associated neovasculature (Kaileh, Vanden Berghe et al. 2007; Srinivasan, Ranga et al. 2007; Lahat, Zhu et al. 2010). These findings further support our observations that vimentin plays a critical role in migration.

Along with IF's, the microfilament actin is known to be a factor in cell shape reconstruction (Moll, Sansig et al. 1991; Takaishi, Sasaki et al. 1997; Tapon and Hall 1997) and regulated by the small GTPases Rac, Rho, and Cdc42 which are known to collectively help in modulating actin polymerization, contraction, and migration (Van Aelst and D'Souza-Schorey 1997; Hall 1998). It has also been linked to influences from vimentin where *in-vitro* labeled actin filaments broke in the presence of polymerizing vimentin (Shah, Wang et al. 1998) and vice versa where activated RhoG, Rac, and Cdc42 induced the collapse of vimentin filaments into the perinuclear region (Valgeirsdottir, Claesson-Welsh et al. 1998; Meriane, Mary et al. 2000; Ridley 2001). Treatment with WFA produced very "spiky" filopodial-like extensions different

from the classic “ruffled” or “widespread lamellipodia” leading edge (Ballestrem, Wehrle-Haller et al. 1998; Ridley, Schwartz et al. 2003). The morphology change could be a reason for the expansion inhibition, as cellular motility has been suggested to be reduced from a lack of lamellipodia formation as shown by dominant negative Rac1 cultured primary mouse epiblast cells which had an average speed reduction of less than half compared to wild-type controls (Sugihara, Nakatsuji et al. 1998). We observed similar effects with Rac1 by inhibiting actin polymerization with the Rac1 inhibitor NSC23766 slowing expansion at 100 μM, and halting expansion at 200 μM. As noted, normal AP development was observed in both cases, though a possible reason is still unknown.

Downie (1976) reported an approximate doubling of the blastoderm radius every 24 hours, with high mitotic indexes within the inner zone, but no cell division in the edge. To maintain confluence we believe the dividing inner zone migrates to the edge, else the epithelial sheet would tear. And, to confirm these earlier findings, we performed a BrdU incorporation assay to label cell nuclei undergoing DNA synthesis, which has since proven to be a more robust proliferation assay than counting mitotic figures. The results here show that the inner zone, is synthesizing DNA. However, BrdU does not directly label cells dividing. It positively labels those cells, which at the time of application of the compound (a pulse), were synthesizing DNA (S-phase). While cytokinesis (the actual dividing of one cell into two) can occur relatively quickly, for example in the span of a few minutes, S-phase can last from several minutes to several hours.(Stern, Fraser et al. 1988; Lequarre, Marchandise et al. 2003; Bao, Zhao et al. 2008; Olivier, Luengo-Oroz et al. 2010). By perfoming a pulse-chase-incubation assay where a sample of embryos were pulsed (exposed to BrdU) for 20 minutes, chased (BrdU diffusion) at room temperature, and then incubated for 8 hours, we saw positive BrdU labeled cells in the

edge which strongly suggests migration from the inner zones to the leading edge.

Also, for such a rapid expansion of the AO to occur, it is likely that 1) the edge cell motility must increase, 2) degradation of the basement membrane is increased.Although Chernoff (1989) reported laminin to be absent from the ventral and basal surfaces of this adhesive edge region, with both becoming progressively more complete closer to the embryo, that study did not notice the gradual appearance of gaps culminating in punctate expression in the edge which we observed. Instead, laminin expression approaching the edge appears to be similar to that observed by Bortier (Bortier, De Bruyne et al. 1989) in the primitive streak where the laminin layer seems to progressively thin out below the future mesoderm cells that are going to de-epithelialize and ingress.

There are several explanations/mechanisms for our observations. The first is that the basal lamina is already present at the start of epiboly, and is torn by increasing tension due to blastoderm expansion. Downie (1976) noticed that expansion runs ahead of cell proliferation for about the first 38 hours, and believed that the cells are stretched to occupy more space, until proliferation is able to relieve the tension. Second, matrix metalloproteinases (MMP's) which degrade ECM proteins may be balancing ECM depositionat the edge to modulate cell motility, as MMP's are known to be involved in wound healing, tissue remodeling, and migration (Madlener, Mauch et al. 1996; Rechardt, Elomaa et al. 2000; Salmela, Pender et al. 2004), and more ECM would likely facilitate migration as cell migration speed has a dependence on substrate ECM composition (Adams and Schwartz 2000; Ridley 2000; Wenk, Midwood et al. 2000; Ridley 2001).. Third, we postulate that as the edge expands it could be depositing ECM, hence the punctate expression, but is polymerized by the advancing inner regions. This is supported by the fact that: 1) no positive laminin stains were seen beyond the leading edge, 2) comparable

immunoflourescent intensities between the TZ and IZ suggesting laminin reorganization, not deposition, is responsible for the different morphologies, 3) progressive thinning of the ECM towards the leading edge.

CONCLUSION

We revisited epiboly in the avian embryo to investigate the phenomenon of collective cell migration. Our goals were to 1) characterize the leading edge of an expanding epithelium in its natural state using epithelial and mesenchymal protein markers, 2) explore the impact of vimentin and actin (two well-known proteins known to be involved in migration) on the leading edge, and 3) answer the decades old question of how cells are added to the leading edge. We have shown that the leading edge of an epithelium (at least in the chick embryo) displays epithelial and mesenchymal traits further supporting the notion of the metastable or "partial" EMT phenotype. The dogmatic mesenchymal protein marker, vimentin, is also not enough to enable cellular migration as its morphology has been shown to be critical. Lastly, as the leading edge migrates it recruits cells from inner regions of the epithelial sheet, though the mechanism is still unknown.

One limitation of using the chick embryo is the difficulty in using in-situ hybridization due to the relatively large tissue area compared to the *Drosophila*, *Xenopus*, or Zebrafish embryo, which limits detailed genetic studies. Also, performing histological studies requires great care to not damage the near monolayer leading edge. However, of all the developmental models the avian is evolutionary closest to mammals, which is also easily accessible. Nevertheless, the results of this study have implications not only in developmental dynamics but more importantly in cancer metastasis and wound healing. Using WFA to affect vimentin in the embryo permits the possibility of using the avian embryo for further cancer studies since WFA has been recognized as a substrate for a multitude of kinase-specific sites including ROCK (Inagaki, Nishi et al. 1987; Ciesielski-Treska, Ulrich et al. 1995; Janosch, Kieser et al. 2000; Goto, Tanabe et al. 2002; Lahat, Zhu et al. 2010) and phosphorylation by ROCK causes vimentin destabilization

(Goto, Kosako et al. 1998; Meriane, Mary et al. 2000). Further epibolic studies should include a comparison of the effects of Y27632 (the ROCK inhibitor) to WFA. Another important follow-up experiment would be to treat embryos with nocodazole, a known microtubule inhibitor, and observe whether the VM morphology is branched or aggregated since VM is known to travel along these fibers. Sufficiently young embryos also possess the remarkable ability to heal "scar-free". Specifically the observed leading edge, unlike adult free edges, does not possess an actin purse string to "pull" the wound closed. Understanding the mechanisms which regulate this natural expansion process could allow the development of "scar-free" healing treatments in adults.

PROTOCOLS

Area Opaca and Blastoderm Fusion

To study EMT and MET at the edge of an expanding blastoderm or area opaca (AO), observing how two edges interact is advantageous. However, explanting an AO punch or blastoderm onto a vitelline membrane with an endogenous embryo (an embryo that was cultured on the membrane from its egg) can cause attachment and visualization problems due to the presence of yolk. This protocol provides an optically clear method of observing both samples.

Materials

Cleaned vitelline membranes (at least 10), see Protocol
Embryos

- *For AO fusion collect embryos as per Area Opaca Punch Protocol*
- *For blastoderm fusion, embryos should be incubated for 2.5 hours*

100 mm plate
100 mm plate with 2.4% agar
Sterile 1x PBS
¼" Whatman paper rings
Cordless pipette
10 mL pipette tip
Transfer pipette
Mini transfer pipette
100 mL baked beaker
Fresh EC culture plates
Kimwipes cut into 1.5" x 1.5" squares

Protocol

1) Culture embryos with ¼" paper rings to the desired developmental stage
2) Fill the 100 mm plate with PBS.
3) Place a clean vitelline membrane ventral side up on the bottom of the 100 mm plate.
4) Transfer the embryo to the cleaned vitelline membrane. This is best done by holding an edge of the paper ring to which the vitelline membrane of the embryo is attached (ventral side up!) with a #4 forceps, submerged in the PBS filled 100 mm plate, and firmly against the plate rim.
5) Shake gently but firmly and slowly. You should notice the forceps scraping the plate. The embryo will gradually begin to peel away from the membrane. KEEP TRACK OF THE VENTRAL SIDE!

6) Continue shaking until the embryo peels off. Allow it settle on the membrane or bottom of the well before discarding the ¼" ring.
7) Use #5 forceps to move the embryo onto the membrane, ventral side up.
8) Gently unfold the embryo if it begins to curl.
9) Take the cordless pipette and 10 mL pipette tip and aspirate the PBS. When a thin film remains, use the transfer pipette and mini-transfer pipette. Kimwipes can then be used to remove the remaining PBS just around the embryo.
10) Gently grab a side of the 9/16" paper ring and transfer to a clean EC Culture plate. The slight amount of PBS remaining (even after the Kimwipes) usually provides enough surface tension to keep the embryo attached.

Area Opaca Punch Protocol

The area opaca (AO) is an expanding epithelial sheet surrounding the area pellucida in the chick embryo and is an excellent near monolayer sheet, which can be observed on its natural subtrate (the vitelline membrane). But, separating it from any influence due to the area pellucida for *in-vivo/in-vitro* like testing is difficult. This protocol provides a means of separating a section of the AO which can be cultured independently.

Materials
9/16" Whatman paper rings
(2) 100 mm plates
2.4% agar in 7 mL aliquots
Sterile 1x PBS
3 mm biopsy punch
Clean vitelline membranes (see Protocol)
Cordless pipette
10 mL pipette tip
Transfer pipette
Mini transfer pipette
100 mL baked beaker
Fresh EC culture plates
Micro-dissection scissors
#2 forceps, trapezoidal tip
(2) #4 forceps
Kimwipes, cut into 1"x1" squares

Protocol
1) Culture embryos using 9/16" paper rings, and incubate for ~2 days.
2) Heat 7 mL of 2.4% agar until liquefied. NOTE: The agar easily flash boils and will pop the cap! Pour the agar into a 100 mm plate and quickly swirl to achieve a uniform layer with few air bubbles. Allow the agar to solidify (~10 minutes).
3) Fill the 100 mm plate to the top with PBS, and place a clean membrane ventral side up in the plate. Use the mini transfer pipette to aspirate any yolk.
4) Gently place an embryo ventral side up into the plate. If it doesn't sink gently press on the ring to push it to the bottom. It is best if the embryo is near the cleaned membrane.
5) Use a 3 mm biopsy punch to extract a piece of the area opaca, by pressing straight down into the agar. Slightly rotate (don't twist) the biopsy punch. Lift straight up very gently. Typically a small section of the AO punch remains attached.

6) Use the micro-dissection to completely detach any remaining sections, cutting normal to the surface.
7) The punch will have several layers: the section of removed agar, the vitelline membrane, the endoderm (if it detaches), and the epiblast. Ideally, the endoderm and epiblast remain intact, however, experimentation has shown that the punch will expand without the endoderm. Take the #2 forceps and remove the agar punch. Then separate the vitelline membrane by grabbing a free edge of the AO punch, and gently peeling it away (a #4 forceps might be needed for extra stability). Keep track with your eye of the ventral and dorsal sides of the punch! Transfer the punch, ventral side up, to the cleaned membrane.
8) Remove the 2 day old embryo.
9) Aspirate the PBS slowly from the plate using the 10 mL pipette, and discard into the baked 100 mL beaker. If the embryo starts to move, then aspirate slower.
10) When only about 20% of the PBS is left, use the transfer pipette to remove the remaining PBS. Take care not to disturb the embryo. Remove as much PBS as possible, by tilting the dish when only a thin layer of fluid is left.
11) Soak up any remaining liquid around the embryo using a Kimwipe.
12) If the embryo is firmly attached to the membrane due to surface tension from the thin layer left on top, then use any of the forceps to gently transfer the embryo to a fresh EC culture plate. If not, then grab opposite sides of the paper ring with two #4 forceps, and lift the sides forming a saddle. Gently transfer to a fresh EC culture plate.
13) Pour the discarded PBS from the 100 mL back into the 100 mm plate. One plate usually lasts for 10+ embryos.
14) Incubate the AO punch for desired time. For the first 3-6 hours, the embryo should attach to the membrane, and not expand. Though, some embryos attach faster than others.

Cleaning Vitelline Membranes

This protocol describes how to clean vitelline membranes for use in area opaca punches and blastoderm fusion.

Materials
100 mm plate
Sterile 1x PBS
(2) #4 forceps
EC Culture plates or 0.6% agar in 100 mm plates
9/16" Whatman paper rings
Kimwipes

Protocol
1) Fill the 100 mm plate with PBS
2) Culture eggs normally (incubation is not necessary), except choose a region where the embryo is not present.
3) Use a #4 forceps to gently scrape away excess yolk.
4) Dip the membrane into PBS.
5) Use a Kimwipe to absorb the excess PBS (this will remove a lot of yolk).
6) Repeat until the membrane is transparent. Note: Two yolk removals is typically sufficient.
7) Place the membrane dorsal side down onto an EC culture plate, or onto a 0.6% agar plate.
8) The membranes have been tested for viability up to one week in a humidified container at 4°C.

Modified Whole Mount Technique – Removal of Paper Ring

Maximizing the flatness of an embryo is important for high quality images. The thin paper ring to which the vitelline membrane is attached is sometimes too thick, causing too many focal planes and "ripples" in the sample surface. However, simply separating the membrane from the ring will remove the tension in the membrane causing it to roll onto the embryo and destroying the sample. This protocol provides a method of removing the membrane while keeping the embryo intact.

Materials
Xacto knife or other easily manipulated razor
Glass slides
Kimwipes, cut into 1"x1" squares
Coverslips
Mounting media
Embryos
#4 forceps, Coverslip forceps

Protocol
1) After preparation of the embryo with fluorescent tags, use a Kimwipe to soak up any excess liquid.
2) Place the embryo on the slide (either ventral or dorsal side up).
3) Use another Kimwipe to remove more liquid. Verify that the sample is "dry". This can be done by looking at the sample level with its surface and noticing "bumps" and "ripples".
4) Use the razor to cut the membrane. The membrane will be firmly attached to the slide, so simply cutting it as though it were paper will likely tear the embryo or move it. Instead, use the knife to make small radial cuts near the internal edge of the paper ring. Continue around the membrane until some of the embryo and membrane are left on the slide, but the ring is detached.
5) Use the forceps to lift the ring, then take another Kimwipe and remove the remaining liquid.
6) ~20 μL of mounting media is needed, and should be placed half on the embryo, half on the remaining vitelline membrane.
7) Apply a coverslip with coverslip forceps and image.

Tips

- Low viscosity mounting media will help to prevent the sample from wrinkling and folding at the edges. DAPI, Permount supplemented with extra xylenes, and BABB are excellent low viscosity medias.
- If the embryo is very large, or if an air bubble is present beneath the blastoderm, add at least 40 μL of mounting media. The extra fluid will help to reduce wrinkling and folding.

"Quick" Assay

Antibody testing using whole embryos is time consuming. Improper fixation, permeabilization, and blocking can lead to poor or no expression despite high antibody affinity. This "quick" assay permits an antibody to be tested in a day rather than several days, using several simultaneous techniques and varying concentrations of antibody.

Materials
(1) 48-well plate
~25 eggs
¼" Whatman filter paper rings
Megacell nutrient media
Fetal Bovine Serum (FBS)
L-glutamine/Streptomycin
60 mm plates
(1) Mini transfer pipette

Protocol
1) Incubate the eggs for ~2.5 hours, and culture using ¼" paper rings.
2) Prepare the culture media. Supplement the Megacell with 10% FBS and 1% L-glutamine/streptomycin. Store at 4°C until needed. NOTE: This media should not be stored overnight. Discard remainder.
3) Add culture media to each well (~400 μL/well).
4) Fill a 60 mm plate with PBS.
5) Shake an embryo off the vitelline membrane in the PBS well used for removing excess yolk from culturing, and suck it into the mini transfer pipette.
6) Transfer the embryo to the 60 mm plate. Clean the embryo by repeatedly aspirating the embryo into the mini transfer pipette and back to the 60 mm plate. After several of these "washes" excess yolk will be removed and the embryo will be in many pieces.
7) Use the pipette to transfer a piece into a well of the 48-well plate. Only a few embryos are necessary to fill all the wells.
8) Incubate overnight. Most of the embryonic pieces will have adhered and spread on the bottom of each well.
9) Fix the cells in each well using desired protocol.
10) Non-specific block, and apply primary and secondary antibodies for 30 minutes each at 4°C, with standard washes of PBS+Azide for 5 minutes as necessary between steps. NOTE: Only ~200 μL/well is needed for each of these steps.

Tips

- Since the cultures are very small and thin, Triton-X is likely not necessary. Though if desired, use a low concentration of Triton-X for 30 minutes at 4°C (0.1% - 0.5%).
- Rocking the samples, as is typically done with whole embryos, will likely detach most of the cultures.
- If methanol fixation is used, 30 minutes to 2 hours is best, with 5 minutes for each rehydration step.

3% Para + Methanol Fixation

Materials
3% Para aliquots
0.5% TritonX-100
1% TritonX-100
Ice cold Methanol

Protocol

1) Thaw an aliquot of 3% para in the 37°C water bath or in the 4°C fridge.
2) Add a sufficient amount of para to each well so the embryo floats. In a 12-well plate this is ~500μL.
3) Rock for 30 minutes at 4°C .
4) Wash twice for at least 10 minutes each on the rocker in PBS+Azide.
5) Add enough TritonX so each embryo floats. Usually, 0.5% TritonX is sufficient. However, if the embryo is very yolky, then 1% TritonX should be used.
6) Repeat Step 4.
7) Place the methanol from the freezer into a bucket of ice, quickly add methanol to each embryo, and immediately place on the rocker at 4°C for 30 minutes. It is important to prevent over fixation by NOT allowing the methanol to warm.
8) Rehydrate using progressive ethanol concentrations of 90%, 70%, 50%, 30%, and 15% for at least 10 minutes each on the rocker.
9) The embryo is now prepared for immunofluorescence.

BrdU Assay

Bromodeoxyuridine (BrdU) replaces a thymidine group when a cell synthesizes DNA (S-phase). It can be used for proliferation studies, both long and short times, as well as cell tracking. It is generally considered non-toxic.

Materials
BrdU
Millipore Water
DNAse
RNA sterile water
BrdU antibodies

Protocol
1) Make a 10 mM stock solution of BrdU in Millipore water. Heat the water in a 37ºC bath to facilitate dissolving of BrdU.
2) Dilute BrdU stock to 10 μM in EC culture media.
3) Pulse for 20 minutes at 37ºC.
4) Chase for 4 hours at room temperature on non-treated EC culture.
5) Follow para/MeOH fixation.
6) Denature DNA with 50 u/mL DNase in RNA sterile water at 37ºC for 20 minutes.
7) Stop reaction by removing DNase, adding PBS + 0.5% PBS Azide, and rocking at 4ºC for 10 minutes.
8) Follow indirect IF protocol.

FIGURES AND TABLES

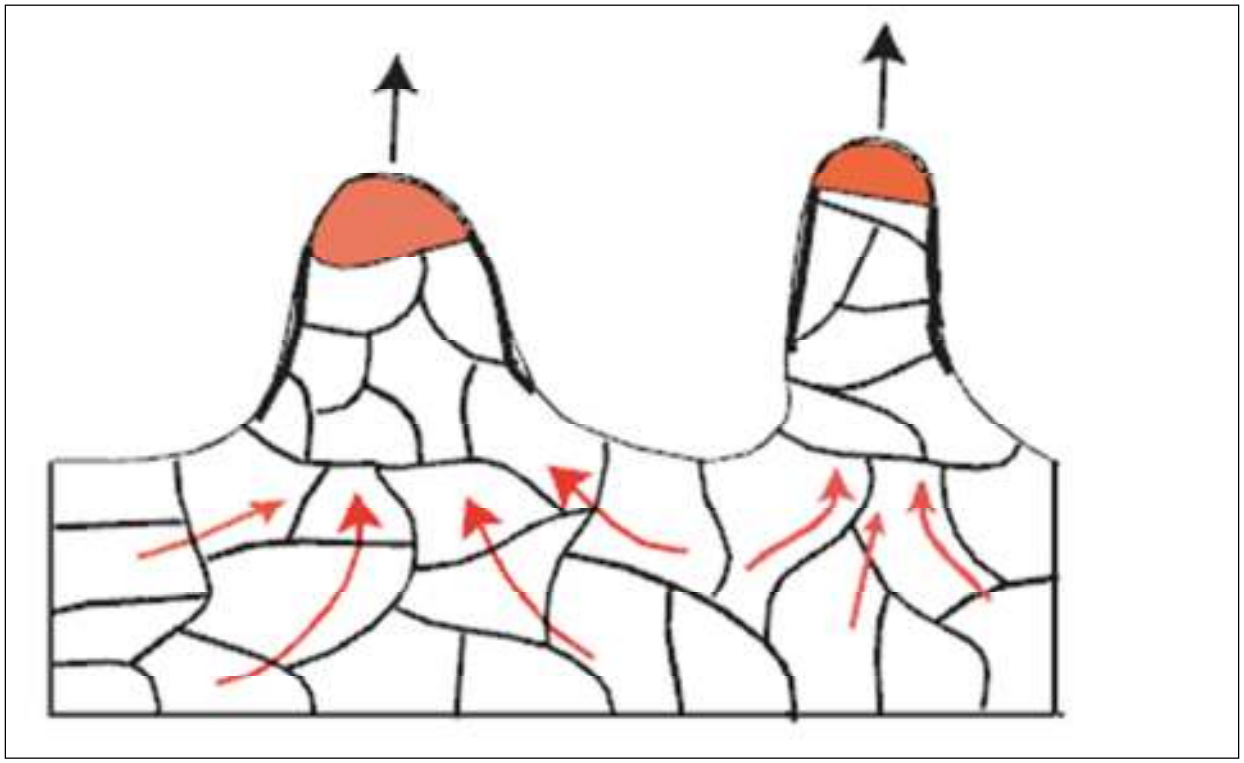

Figure 1: Formation and growth of lamellipodia at a leading epithelial edge. A cell culture expands onto the surrounding substrate in the form of cell columns, with leader cells (red tips) moving fastest forward, dragging their neighbors by means of cytoskeletal scaffolds (heavy black lines) and strong cell– cell cadherin contacts. The continuity of the moving front is always maintained so that the leader cells do not dissociate from their neighbors. Behind the moving front, a collective cell motion (red arrows) feeds the column with cells (Gov 2007).

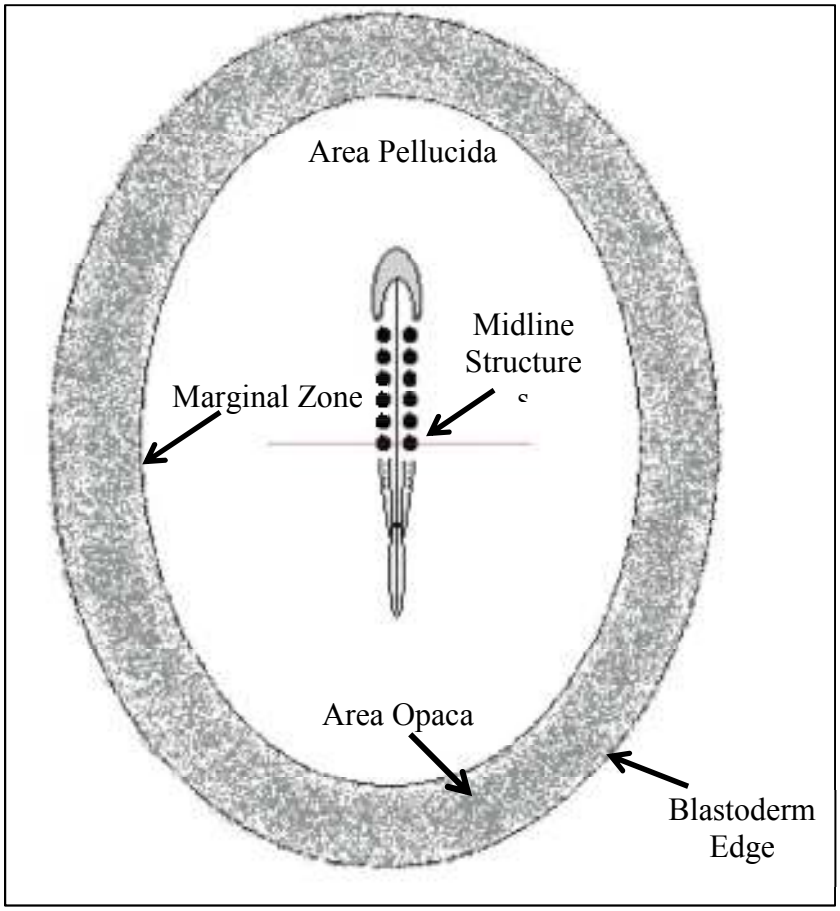

Figure 2: Schematic of a ~24 hour chick embryo. The inner zone where the midline structures (i.e. somites, head fold, neural tube, etc…) are present is called the area pellucida. Separating the area pellucida from the area opaca is a thin delineation called the marginal zone. The entire embryo rests and expands on an *in-ovo* deposited substrate called the vitelline membrane. (http://www.biomedical-engineering-online.com/content/9/1/19/figure/F1?highres=y)

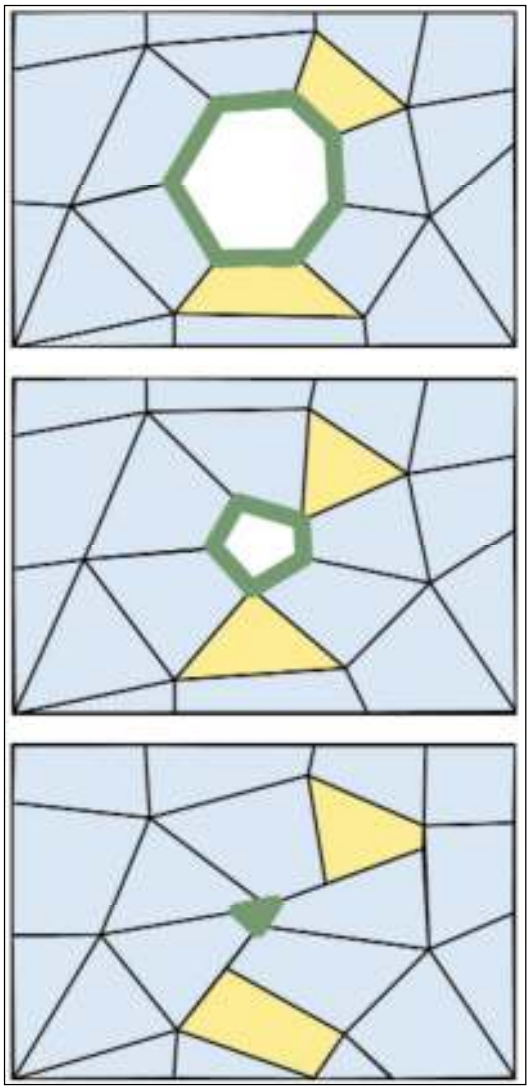

Figure 3: Cell-shape changes and shuffling occurring during repair of an epithelial tissue culture wound. As an epithelial wound repairs (from top to bottom), cells with a margin at the leading edge (green) change their shape and can rearrange their neighbor–neighbor relationships such that they leave the front row (for example, cells marked in yellow). (Jacinto, Martinez-Arias et al. 2001)

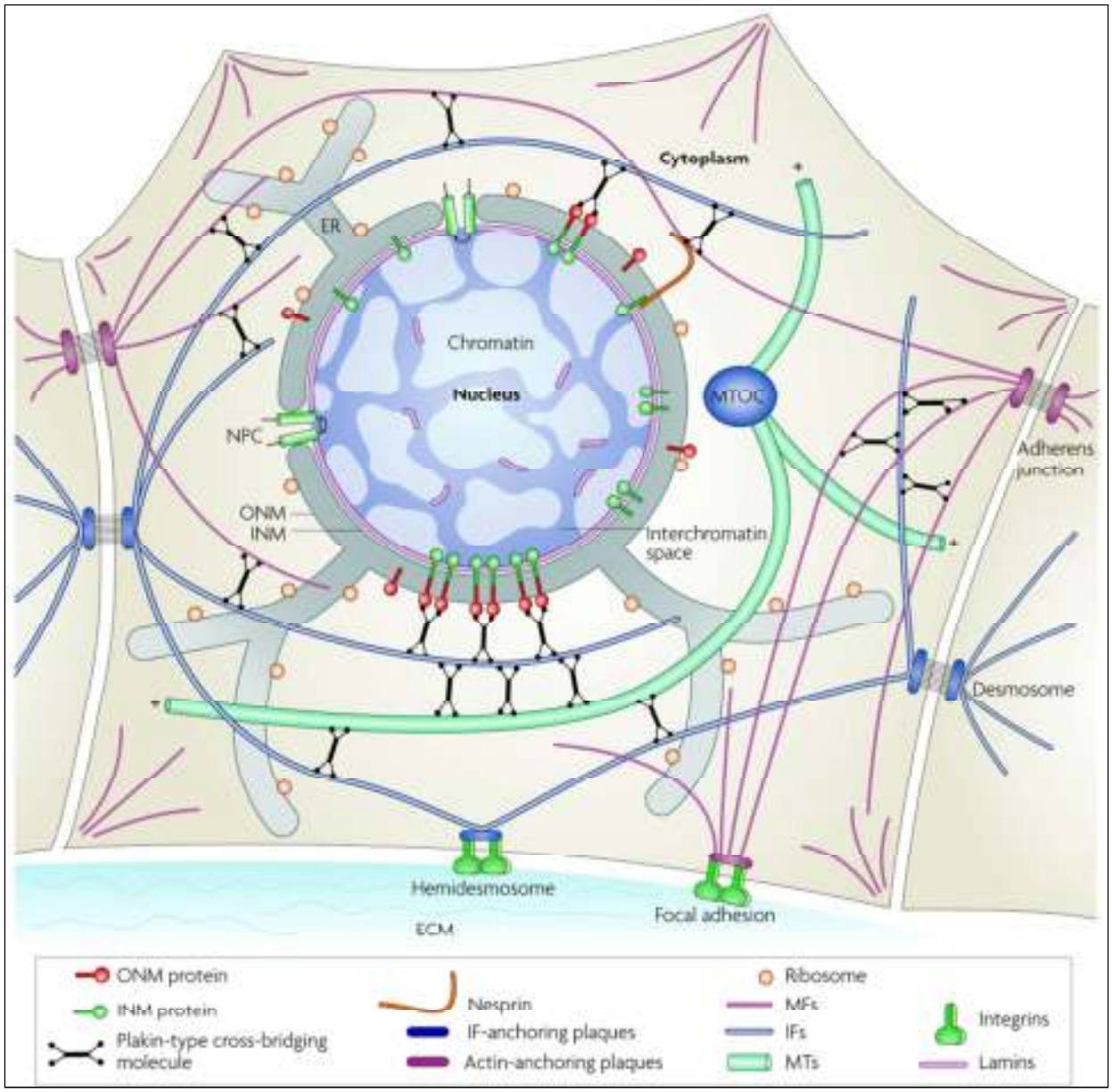

Figure 4: In the hypothetical epithelial cell depicted, the three key filament systems of the cytoskeleton, microfilaments (MFs), microtubules (MTs) and intermediate filaments (IFs), are connected to each other by dimeric complexes of plakin-type molecules such as plectin and BPAG1. In addition, a multitude of MT-associated proteins and actin-binding proteins, including motor proteins, are thought to increase the complexity of these interactions. IFs are coupled to IF-anchoring plaques of cell–cell junctions (desmosomes) by desmoplakin, a prototype plaque molecule (plakin), and to those of cell–matrix junctions (hemidesmosomes) by plectin and BPAG1. The transmembrane proteins that mediate the contact with the neighboring cells and with the extracellular matrix (ECM) are desmosomal cadherins and integrins, respectively. IFs are furthermore coupled to the outer nuclear membrane (ONM), whereas the MF system is anchored to the nucleus. On the inner side of the nuclear envelope, a layer of nuclear IF proteins (lamins) is attached to pores and inner nuclear membrane (INM) proteins as well as to chromatin. The membrane proteins of the INM might be linked to those of the ONM and thereby provide a mechanical continuum reaching from the ECM to chromatin. The number of newly identified INM and ONM proteins is increasing steadily and is represented here only in a schematic manner. ER, endoplasmic reticulum; MTOC, microtubule-organizing centre; NPC, nuclear pore complex. (Herrmann, Bar et al. 2007)

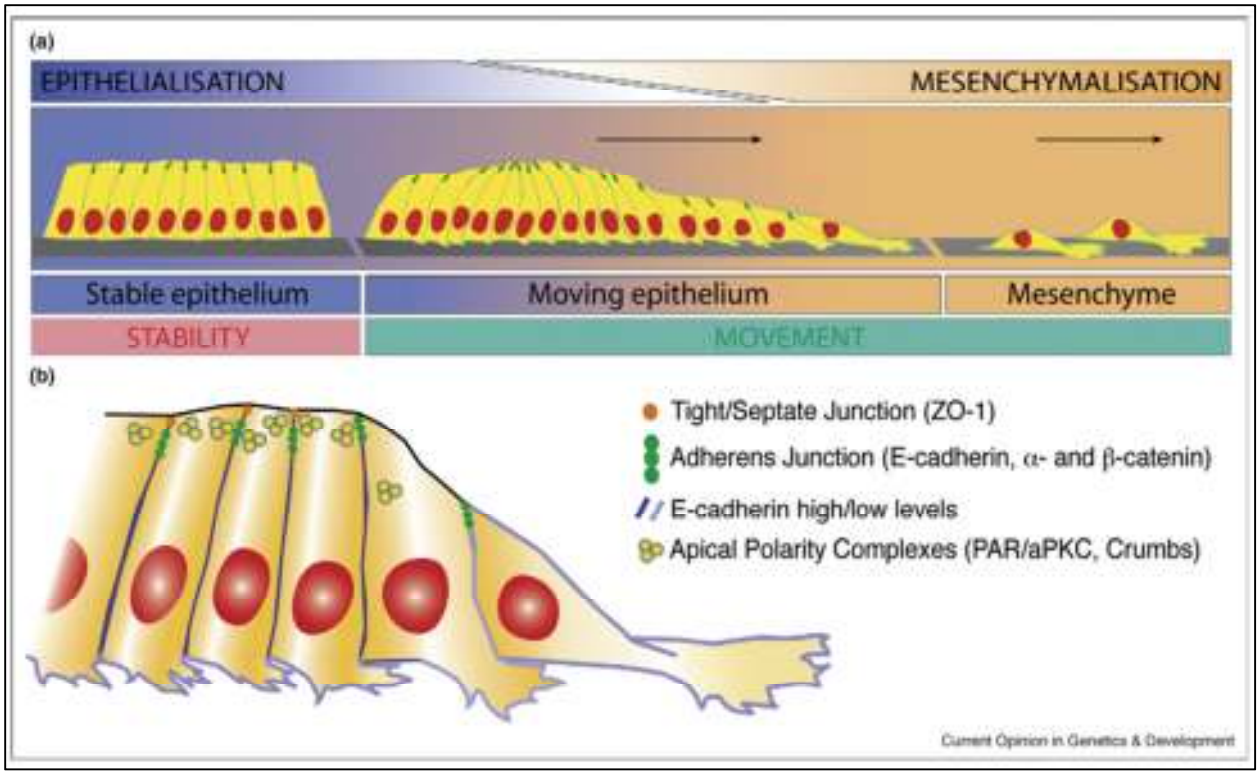

Figure 5: Collective migration of an epithelium with local, graded EMT. (a) Schematic highlighting the different morphological cellular states encountered in EMT. On the left, the apico-basally polarized epithelium is highly ordered and static. On the right, two individually migrating cells depict the flattened, labile and dynamic mesenchymal state. In between, a theoretical example of collectively migrating cells is represented. It consists of a group of apico-basally polarized cells exhibiting local melting of the epithelial organization. This intermediate motile state is controlled by equilibrium between epithelializing and mesenchymalizing cues. The direction of migration is depicted (black arrow). (b) Model of the polarized organization of a collectively migrating group of cells. Numerous cells have the characteristics of a true epithelium. Leading-edge cells undergoing different degrees of EMT develop dynamic membrane protrusions as lamellipodia and filopodia. Depending on the extent of their EMT, they exhibit a loss of tight junctions markers as ZO-1, a reduced level of adhesion proteins as E-cadherin, a-catenin and b-catenin. The apical polarity complexes are also delocalized or reduced (Revenu and Gilmour 2009).

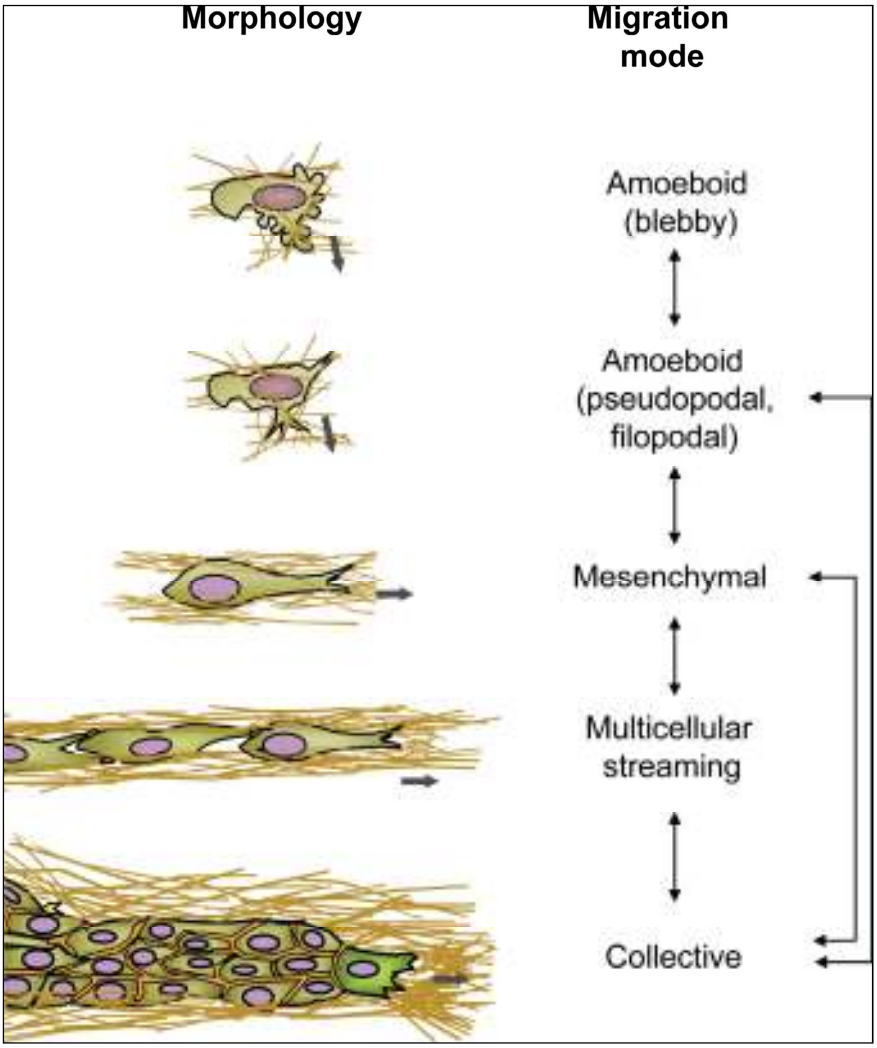

Figure 6: Cell morphologies, migration modes, and transitions. The nomenclature of interstitial migration modes is based on typical cell morphology (rounded or spindle-shaped) and pattern (individual, loosely connected, or collective). Each migration mode is governed by a set of molecular mechanisms, the regulation of which can change the style of migration. Most widely studied examples for alterations of migration mode are the mesenchymal-to-amoeboid transition or the collective-to-individual transition. The thick gray arrows indicate the direction of migration (Friedl and Wolf 2010).

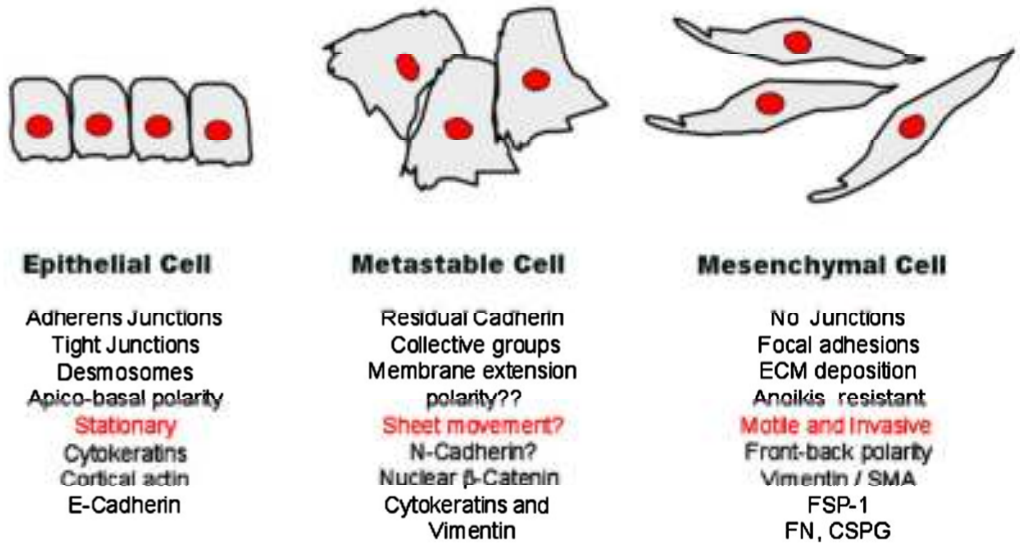

Figure 7: The metastable cell phenotype: a hybrid cell showing both epithelial and mesenchymal traits. These cells are summarized here, in conjunction with their epithelial and mesenchymal counterparts. The term metastable was introduced at the meeting by Pierre Savagner, who showed evidence of epithelial and mesenchymal Rac localization within the same cells (Lee, Dedhar et al. 2006).

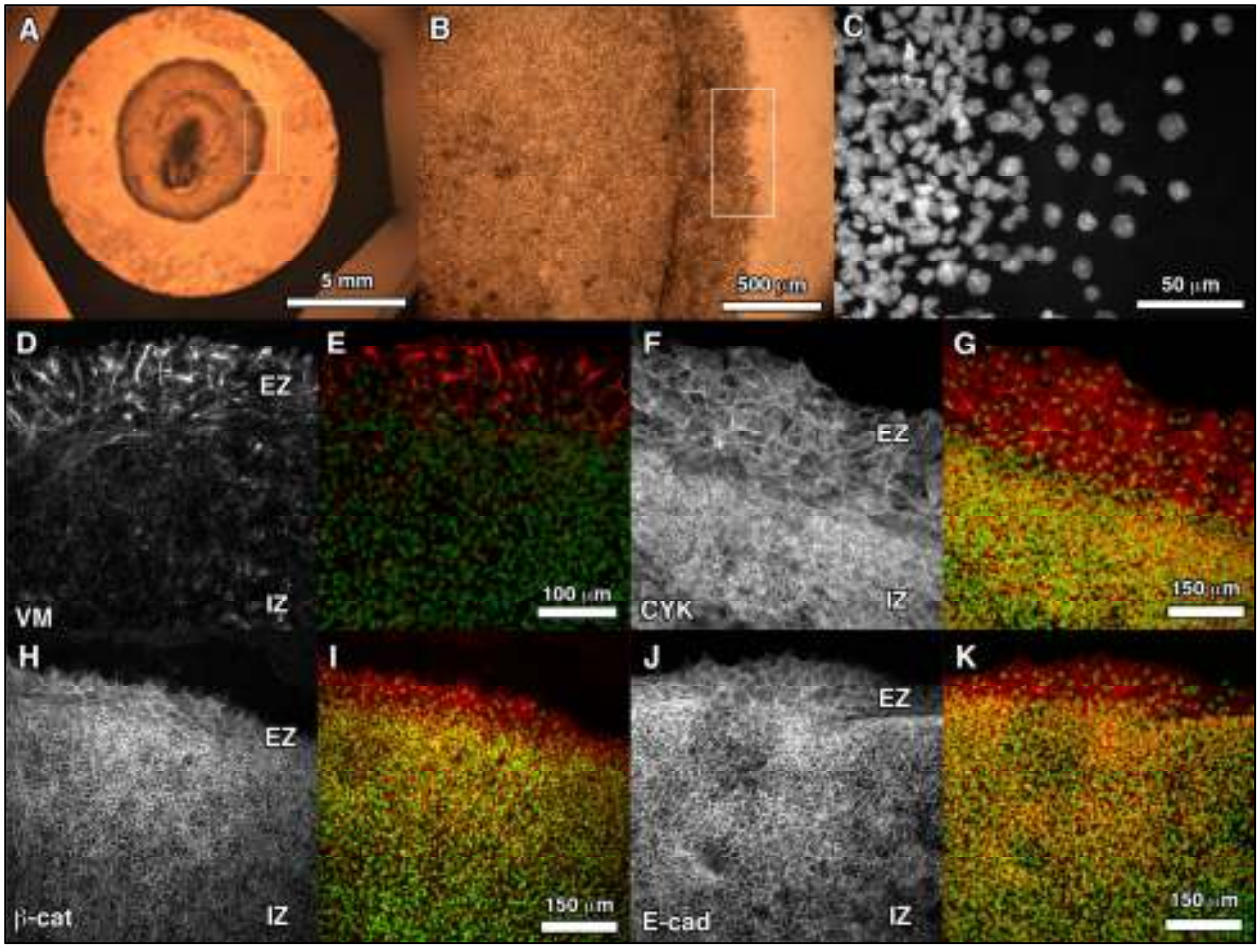

Figure 8: A-C: progressive close-ups of the area of interest of the quail embryo indicated by the white box. B is a representative close-up of A; C is representative close-up of B. D-M: 20x representative immunoflourescent images of each protein and each protein + nuclei merge, (D-E) vimentin (VM); (F-G) keratin (CYK); (H-I) β-catenin (β-cat); (J-K) E-cadherin (E-cad). EZ (edge zone); IZ (inner zone). The scale in image M is the same for images F-M.

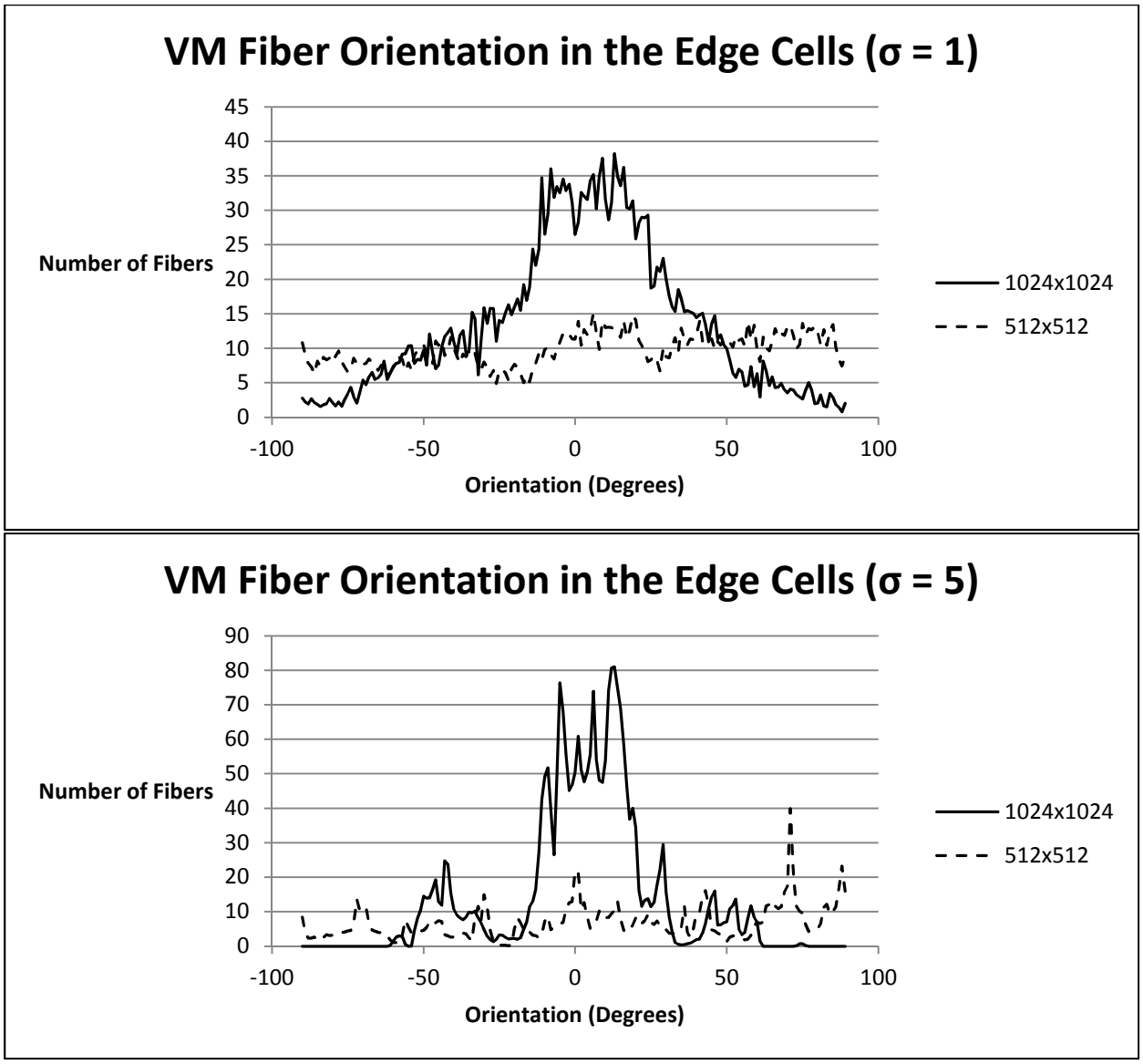

Figure 9: VM fiber histograms in the leading edge cells. An orientation of 0 indicates a horizontal fiber. Two groups of leading edges with resolutions of 1024x1024 and 512x512 are shown for each of the Gaussian windows (σ =1, σ = 5). The "smoother" window (σ = 5) shows that the fibers are primarily oriented between ~ ±25º, with smaller peaks centered around ±50º for the 1024x1024 resolution group. The lower resolution group has a "dispersed" distribution.

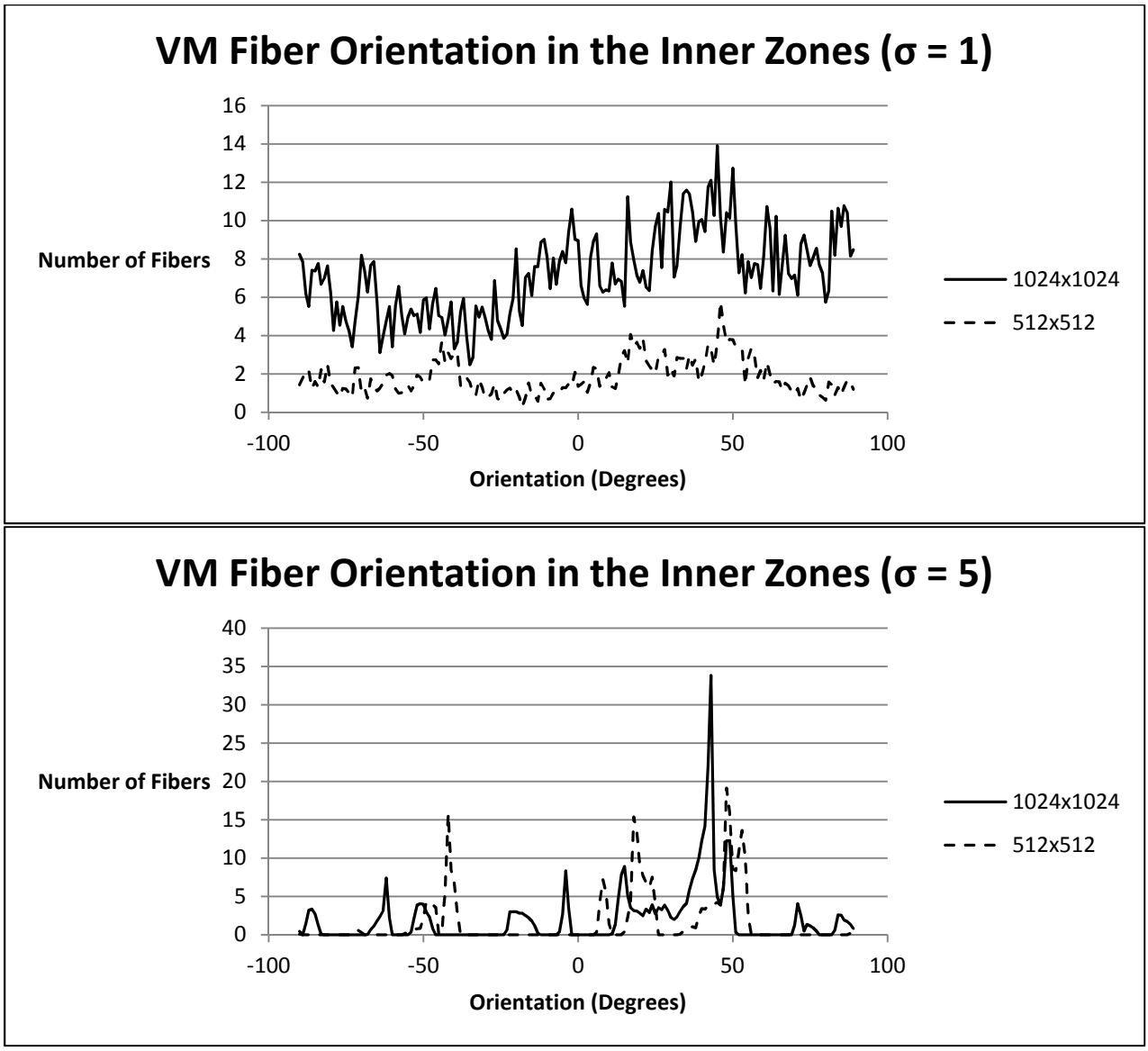

Figure 10: VM fiber histograms in the inner zone cells. An orientation of 0 indicates a horizontal fiber. Two groups of leading edges with resolutions of 1024x1024 and 512x512 are shown for each of the Gaussian windows (σ =1, σ = 5). The "rough" window (σ = 1) shows "dispersed" orientations suggesting random fiber directions for both resolutions. Smoothing the data (σ = 5) shows spikes of orientation preference around ±50º.

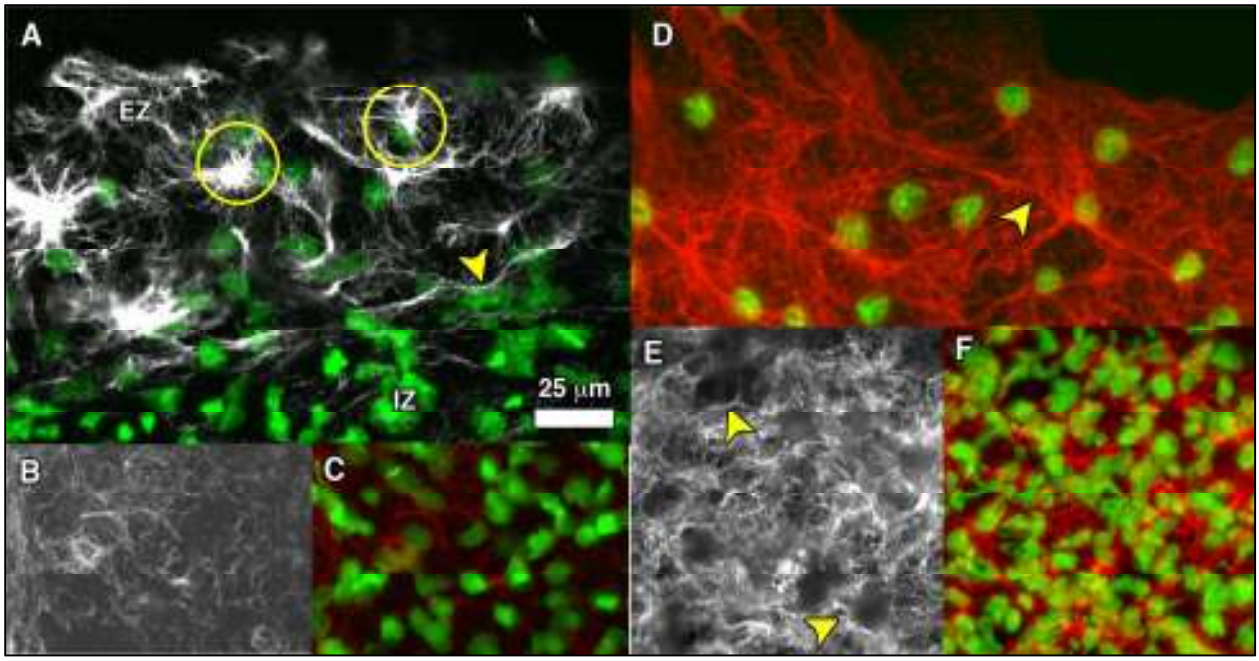

Figure 11: 60x representative images of vimentin and keratin. A: co-localization of vimentin and nuclei in the EZ. The arrowhead shows a thick vimentin filament, and the circles show vimentin "clusters". B-C: vimentin IZ (B) and vimentin IZ + nuclei (C). The circle shows a region of vimentin "squiggles". D: keratin EZ + nuclei. The arrowhead indicates a keratin fiber. Notice the "web-like" network throughout the edge. E-F: keratin IZ (E) and keratin + nuclei (F). The arrowheads denote keratin fibers.

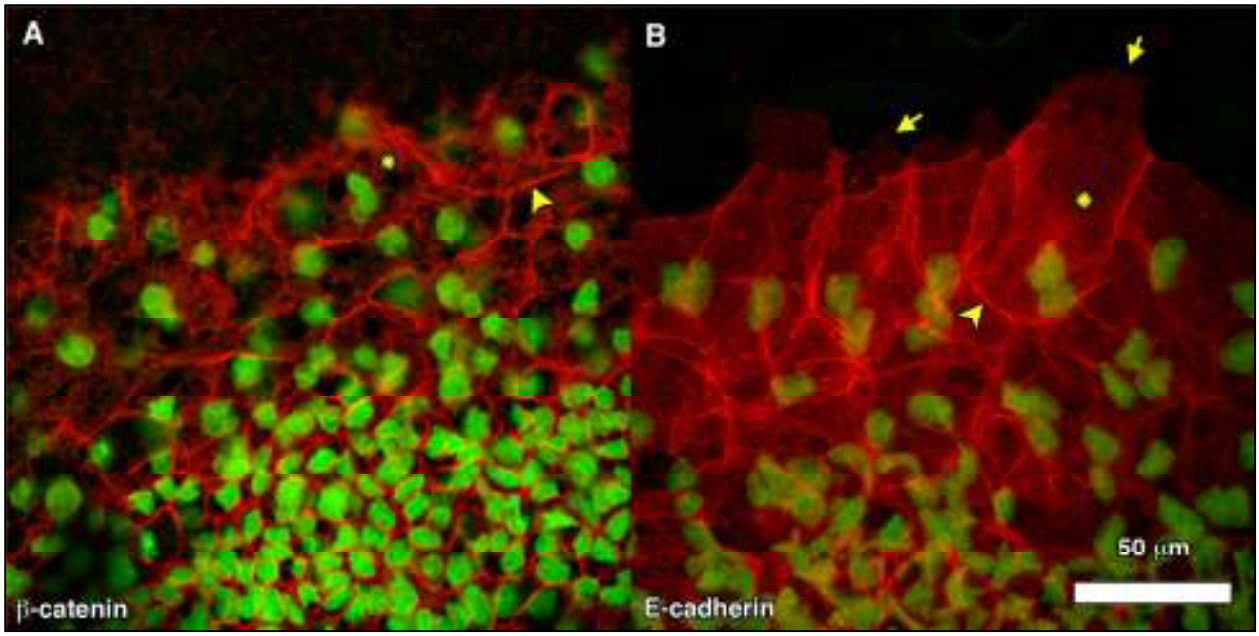

Figure 12: 60x representative EZ images of β-catenin (A) and E-cadherin (B). The arrowheads show cell borders; the arrows indicate lamellipodia and filopodia; the asterisks denote a region of cytoplasmic diffusion of each protein.

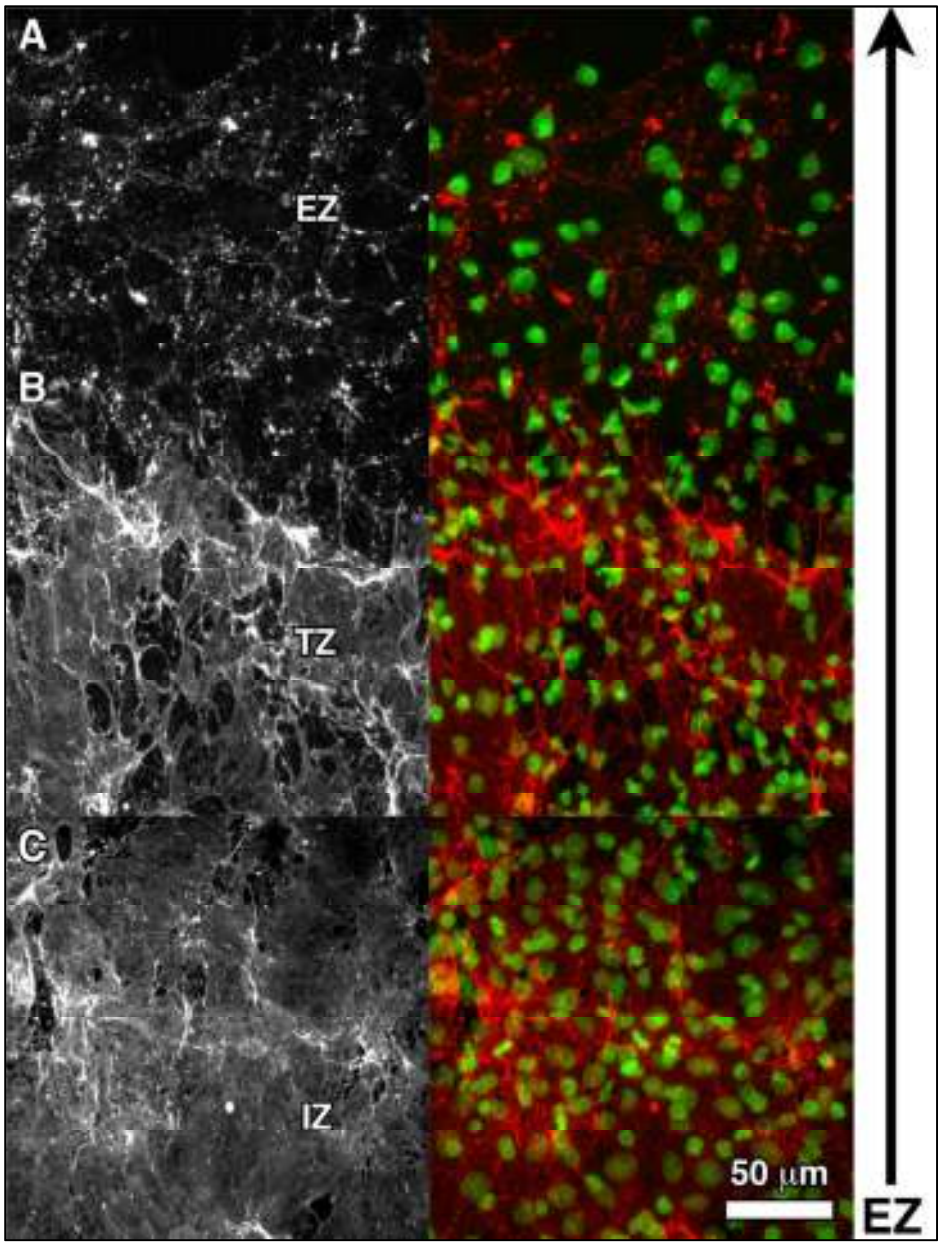

Figure 13: Panoramic view of 60x laminin images from the (A) inner zone (IZ), (B) transition zone (TZ), and (C) edge zone (EZ). The arrow denotes the direction of increasing "gaps" in laminin towards the edge.

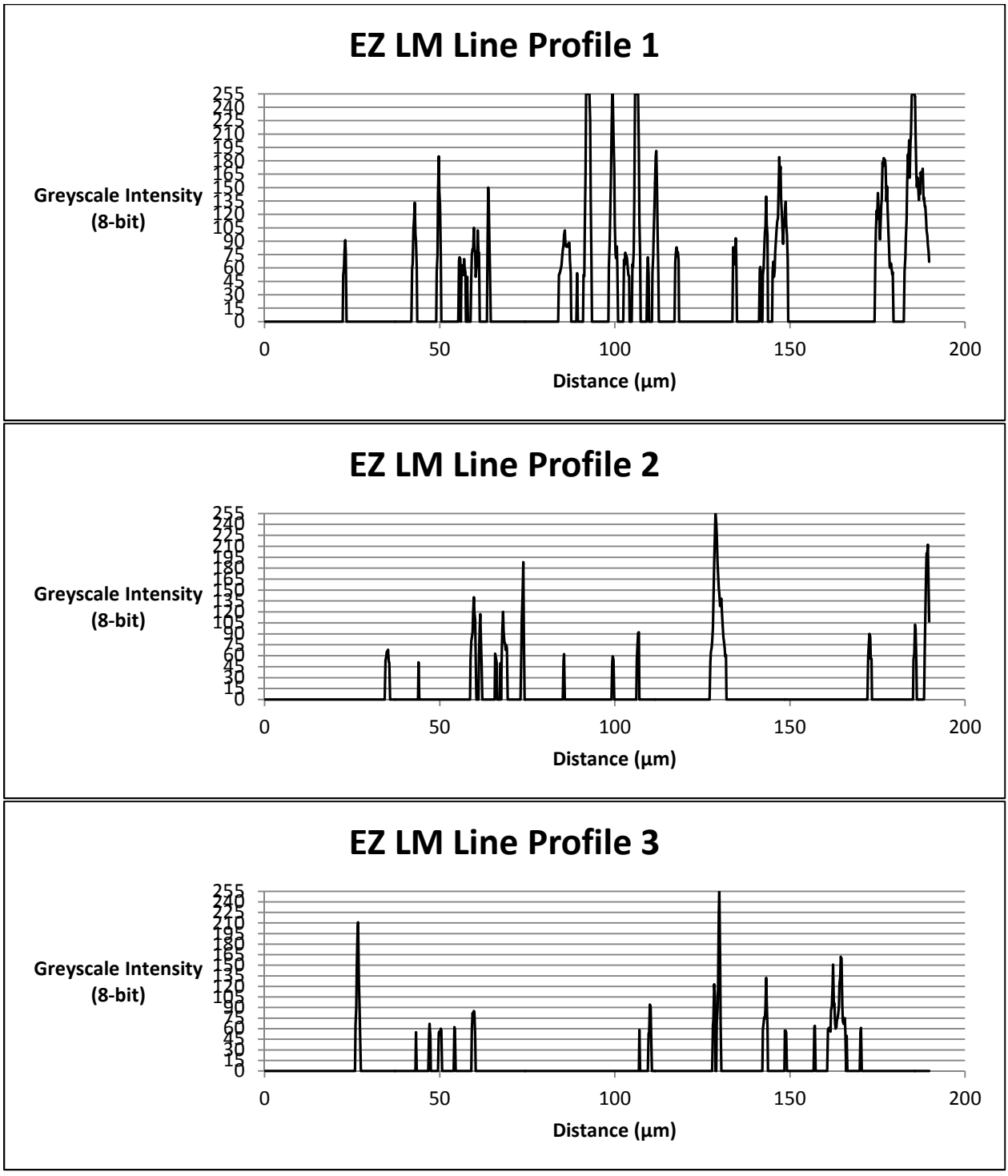

Figure 14: Column averaged pixel intensity line profile of the edge zone (EZ) in Figure 12. Each of the profiles shown are spaced 256 pixels apart (~50 µm). An intensity of 0 denotes a "gap" or "hole", and 255 is saturation. The "gaps" are separated by narrow high intensity sometimes saturated regions indicative of the bright punctate spots in the EZ.

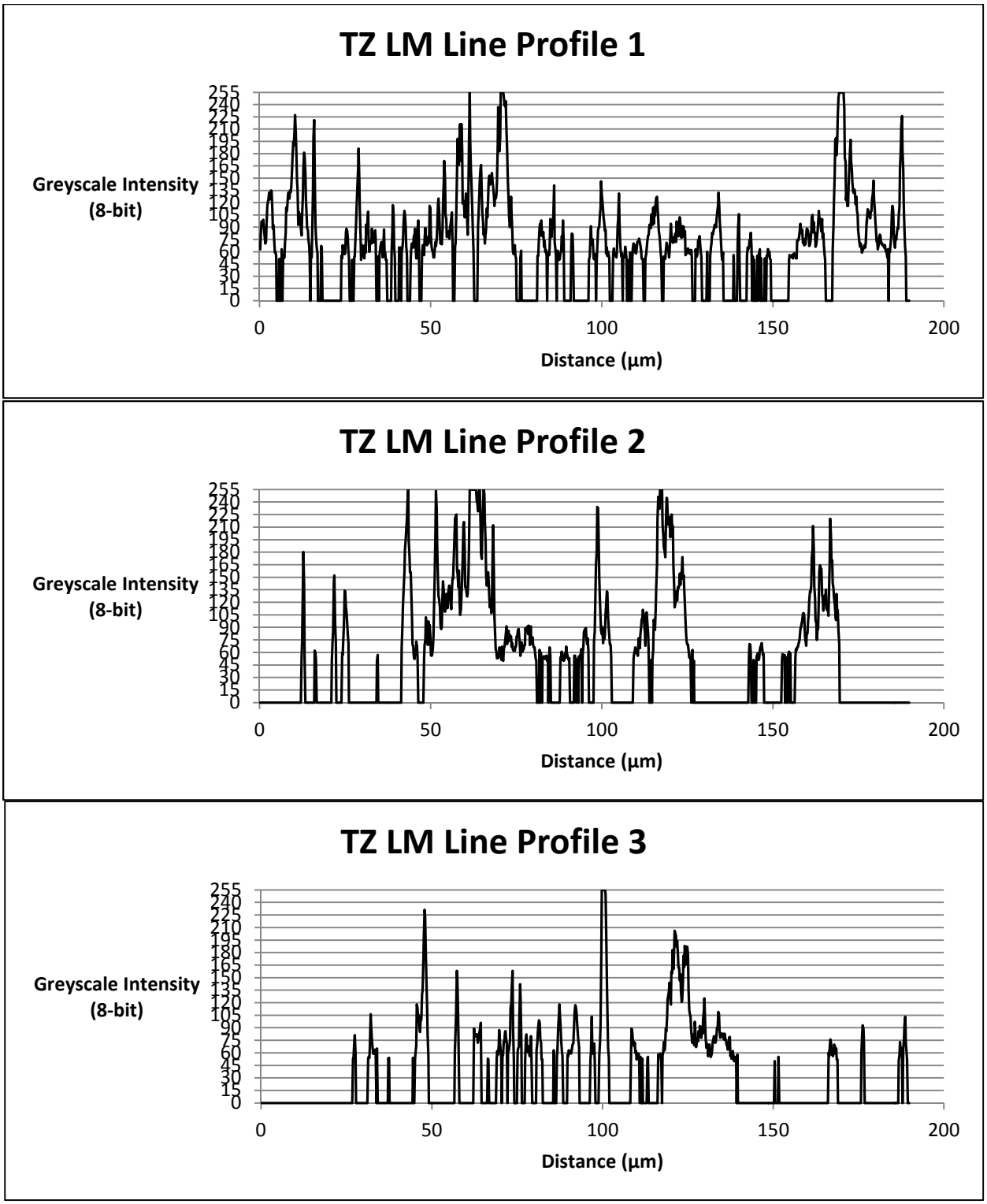

Figure 15: Column averaged pixel intensity line profile of the edge zone (TZ) in Figure 12. Each of the profiles shown are spaced 256 pixels apart (~50 µm). An intensity of 0 denotes a "gap" or "hole", and 255 is saturation. The size and number of "gaps" have decreased compared to the EZ.

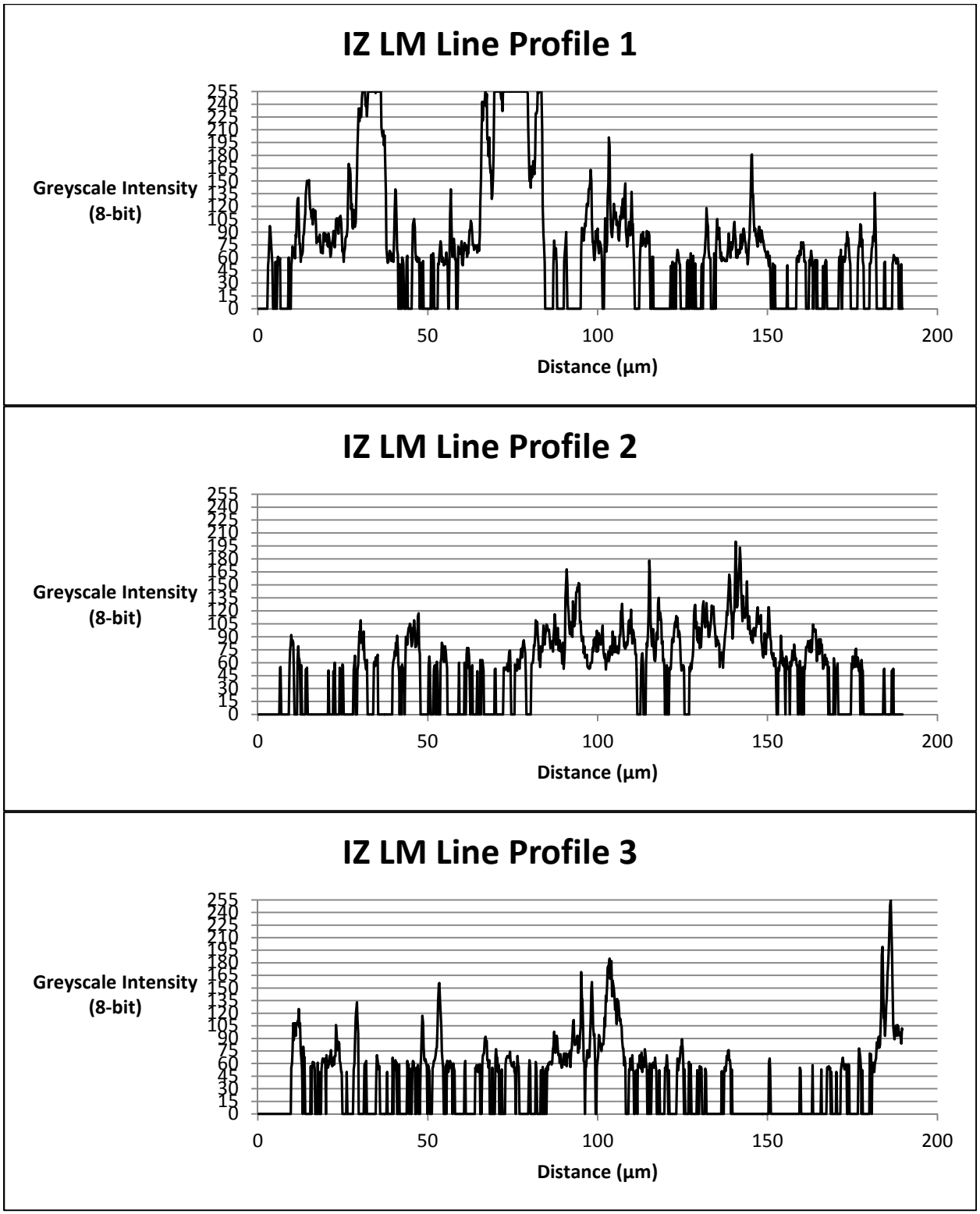

Figure 16: Column averaged pixel intensity line profile of the edge zone (IZ) in Figure 12. Each of the profiles shown are spaced 256 pixels apart (~50 µm). An intensity of 0 denotes a "gap" or "hole", and 255 is saturation. The intensity at each of the points are closer in value to each other than the TZ, though there are still very small "gaps" present which are not visually apparent.

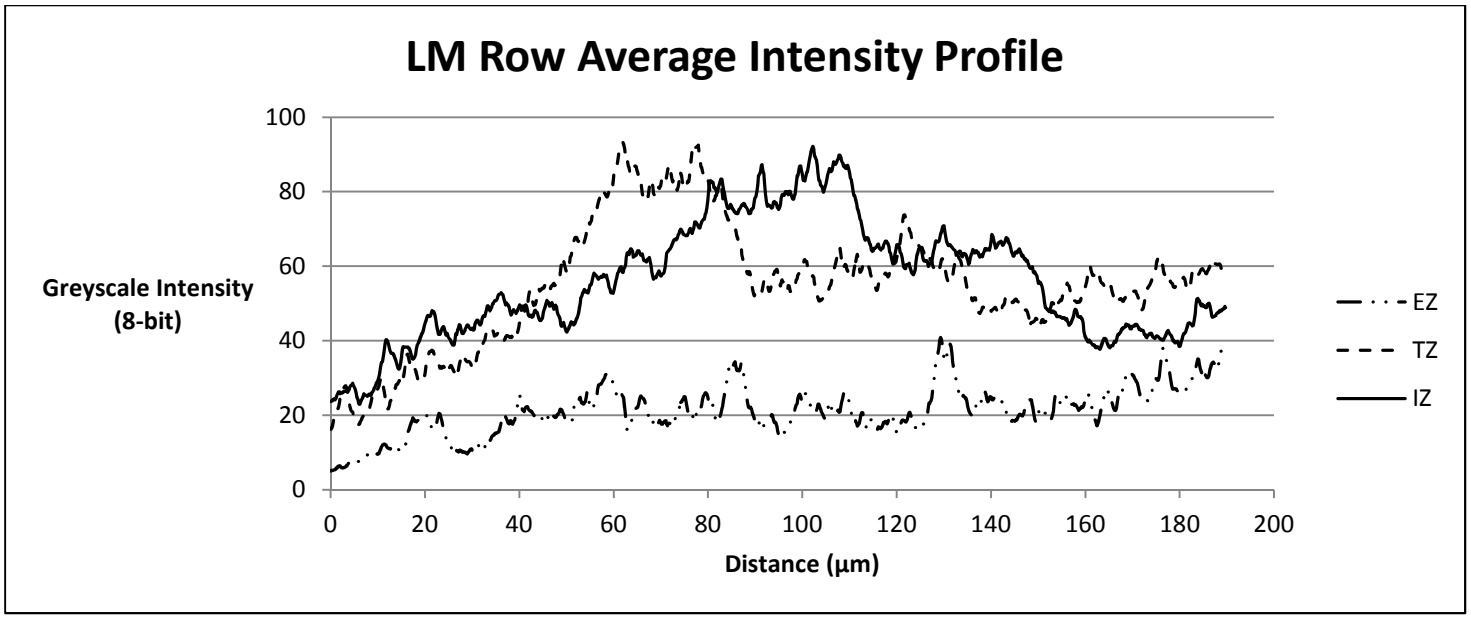

Figure 17: Row average intensity profile of the edge zone (EZ), transition zone (TZ), and inner zone (IZ) of the LM panoramic image in Figure 12. Distance is measured from the top of the image (towards to the leading edge) as 0 and increasing in magnitude towards the bottom of the image (towards the inner regions). An pixel intensity of 0 shows no immunofluorescence and a pixel intensity of 255 shows saturation. The TZ and IZ have average intensity profiles of 55.1 ± 16.1 and 55.9 ± 16.0 which suggests equal amounts of laminin in both zones.

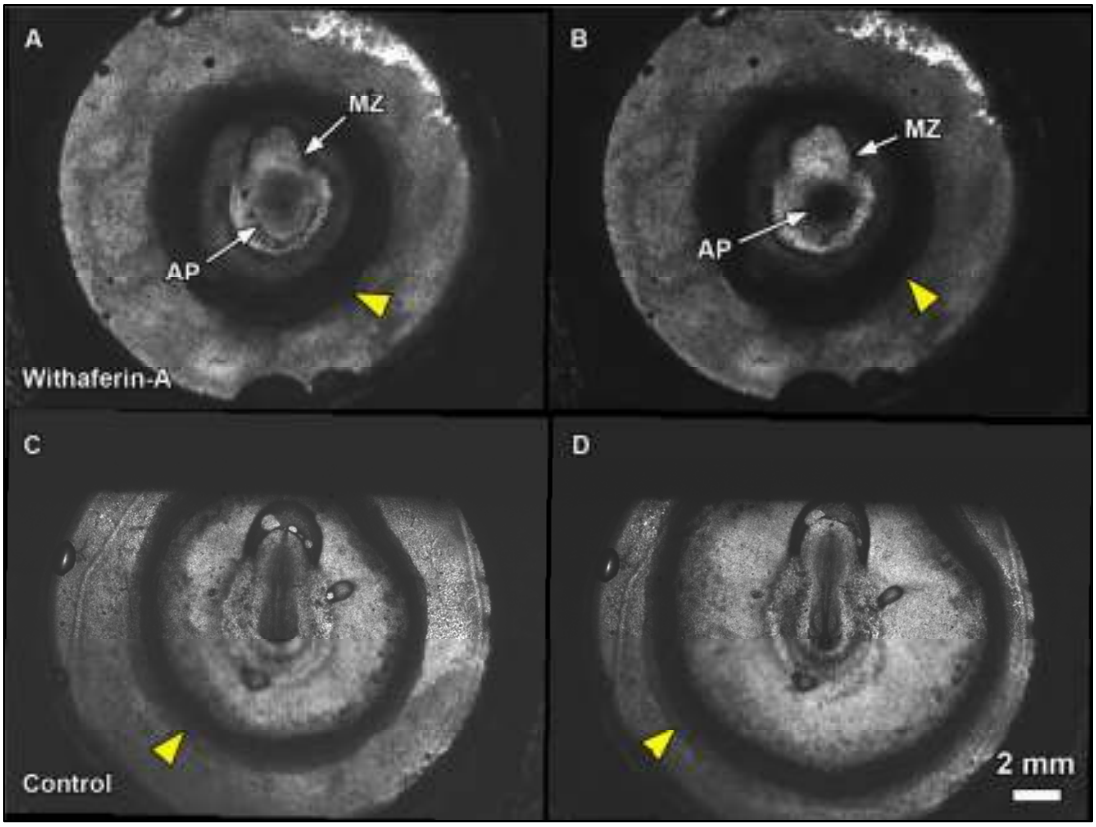

Figure 18: Withaferin-A Expansion Inhibition. AP (area pellucida), MZ (marginal zone). Yellow arrow heads denote edge of blastoderm. Time between frames ~3.5 hours.

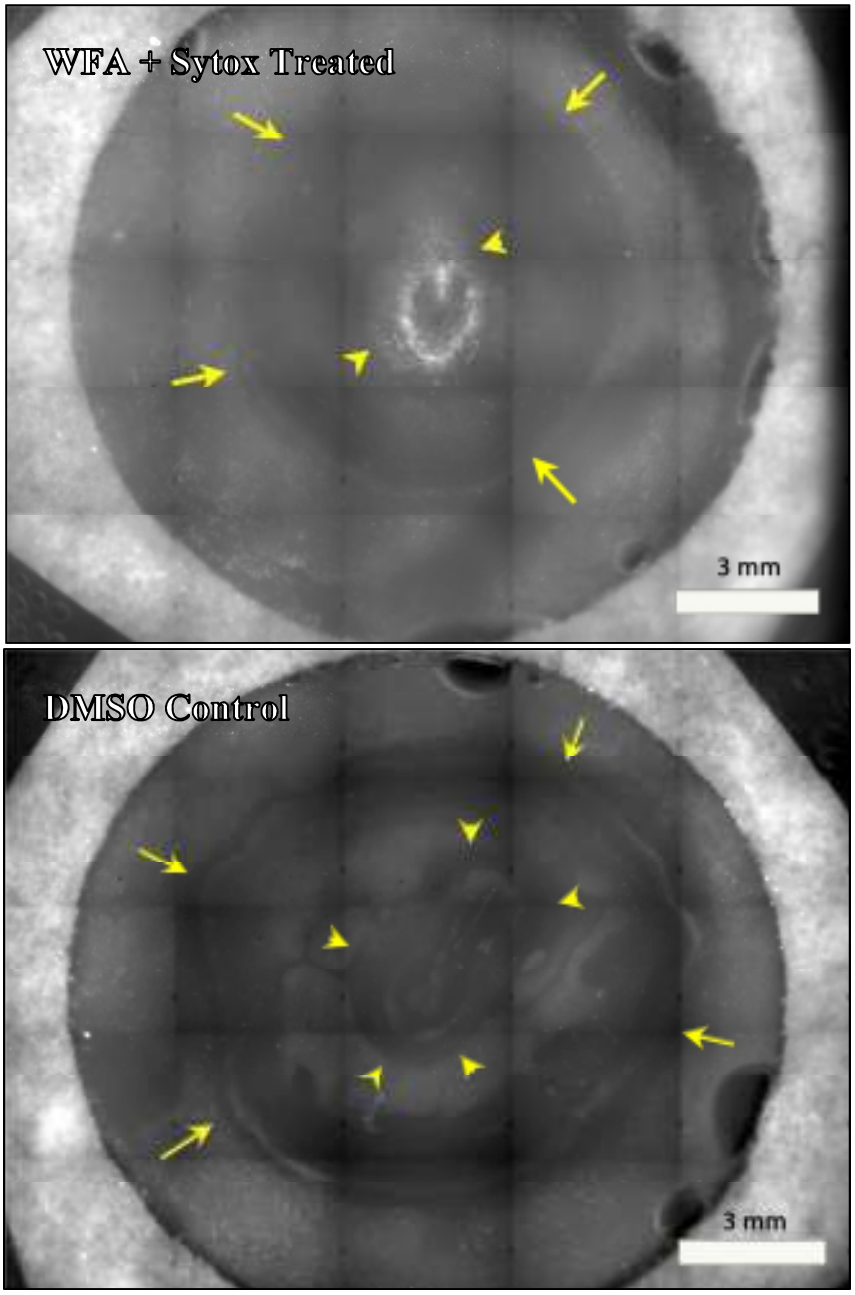

Figure 19: Representative images of a 50 µM WFA + 1 µM Sytox treated embryo and DMSO control. Arrowheads show the edge of the AP; arrows show the blastoderm edge. The bright speckled area denoted by the arrowheads in the WFA + Sytox treated specimen is positive Sytox staining. No apparent Sytox staining was found in the controls.

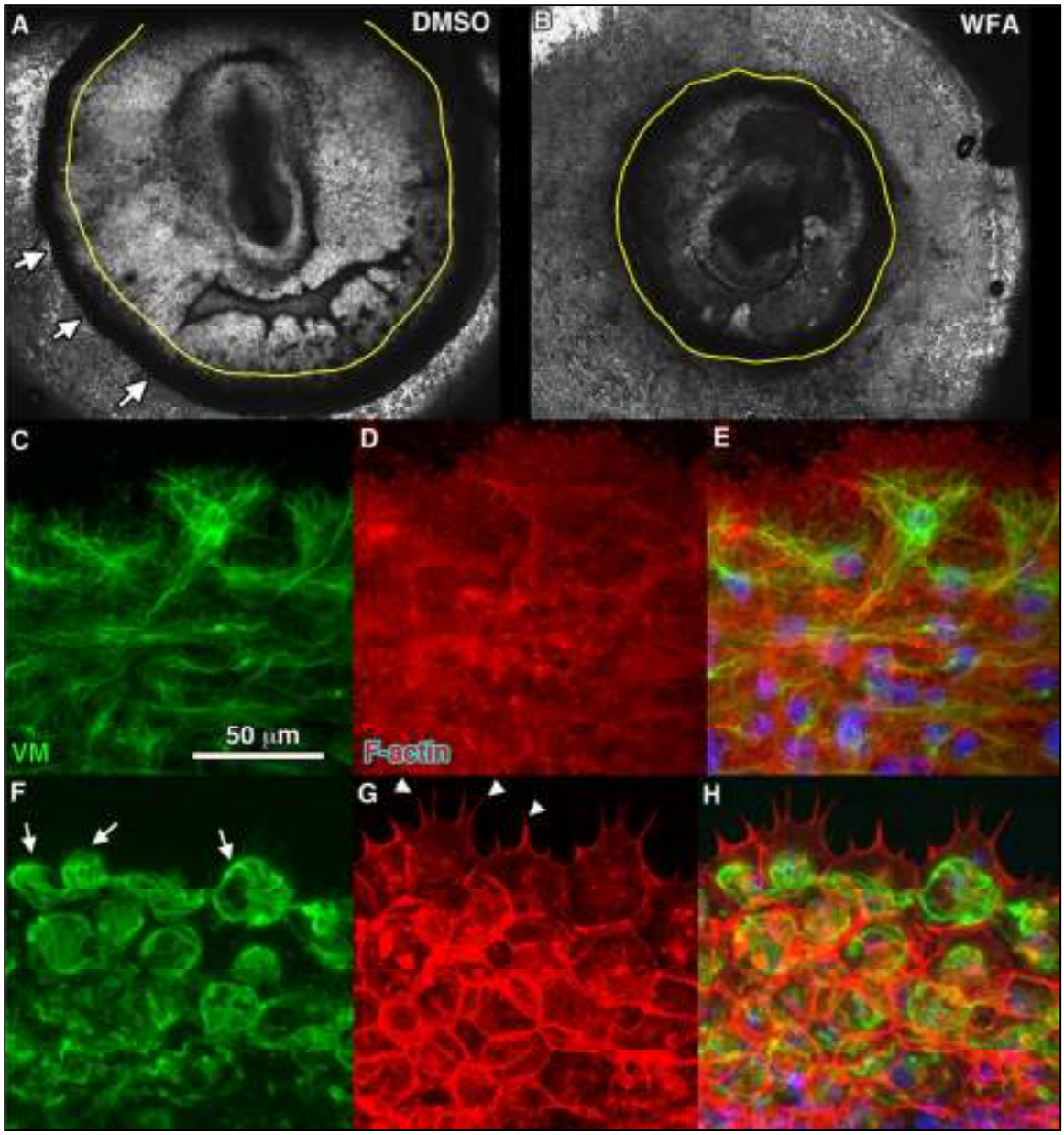

Figure 20: Effects of a vimentin-targeting drug, Withaferin A (WFA). (A) Control embryo undergoes normal epiboly. Yellow line represents the edge of the blastoderm at the initial time point, and the white arrows indicate the location of the edge after 4 hours of incubation. (B) Epiboly in a representative WFA-treated embryo is completely blocked during the same time-course. (C-H) High-resolution (60X) confocal images of representative control (C-E) and WFA-treated (F-H) embryo at the blastoderm edge. Note the retracted appearance of vimentin filaments in WFA-treated edge cells (F, arrows) and the emergence of spiky filopodial-like protrusions, as shown by rhodamine-phalloidin staining of F-actin (G, arrowheads). (E,H) Merge of vimentin, F-actin, and DAPI nuclear staining.

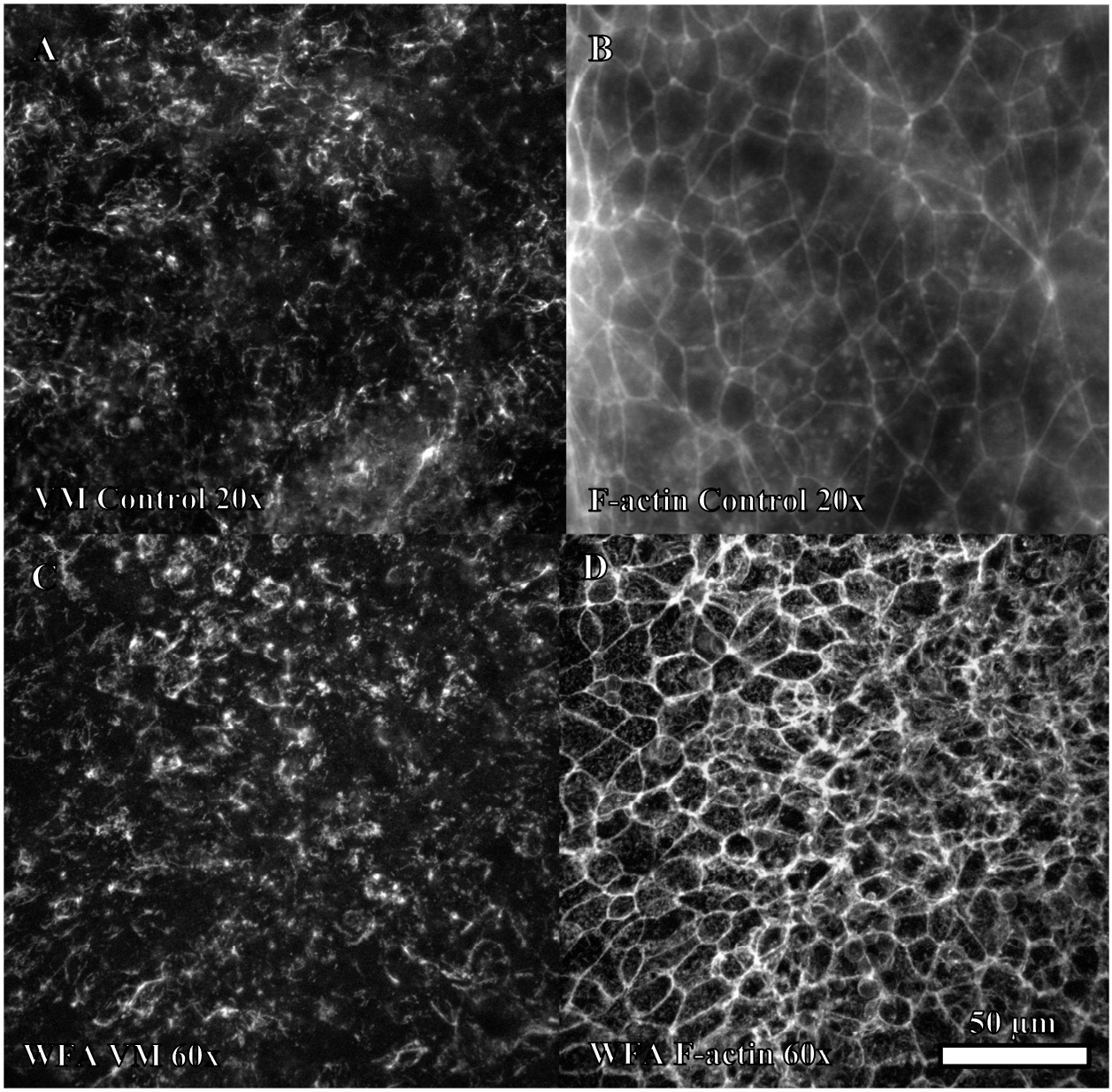

Figure 21: Inner regions of control and WFA treated samples. The controls are 20x, the WFA are 60x. Scale bar is 50 µm for C and D. NOTE: No scale is available for A and B. F-actin morphology (B, D) shows well-defined cell borders for both the control and WFA treated samples. The inner VM zones (A, C) have the reminiscent VM squiggles shown in Figure 11.

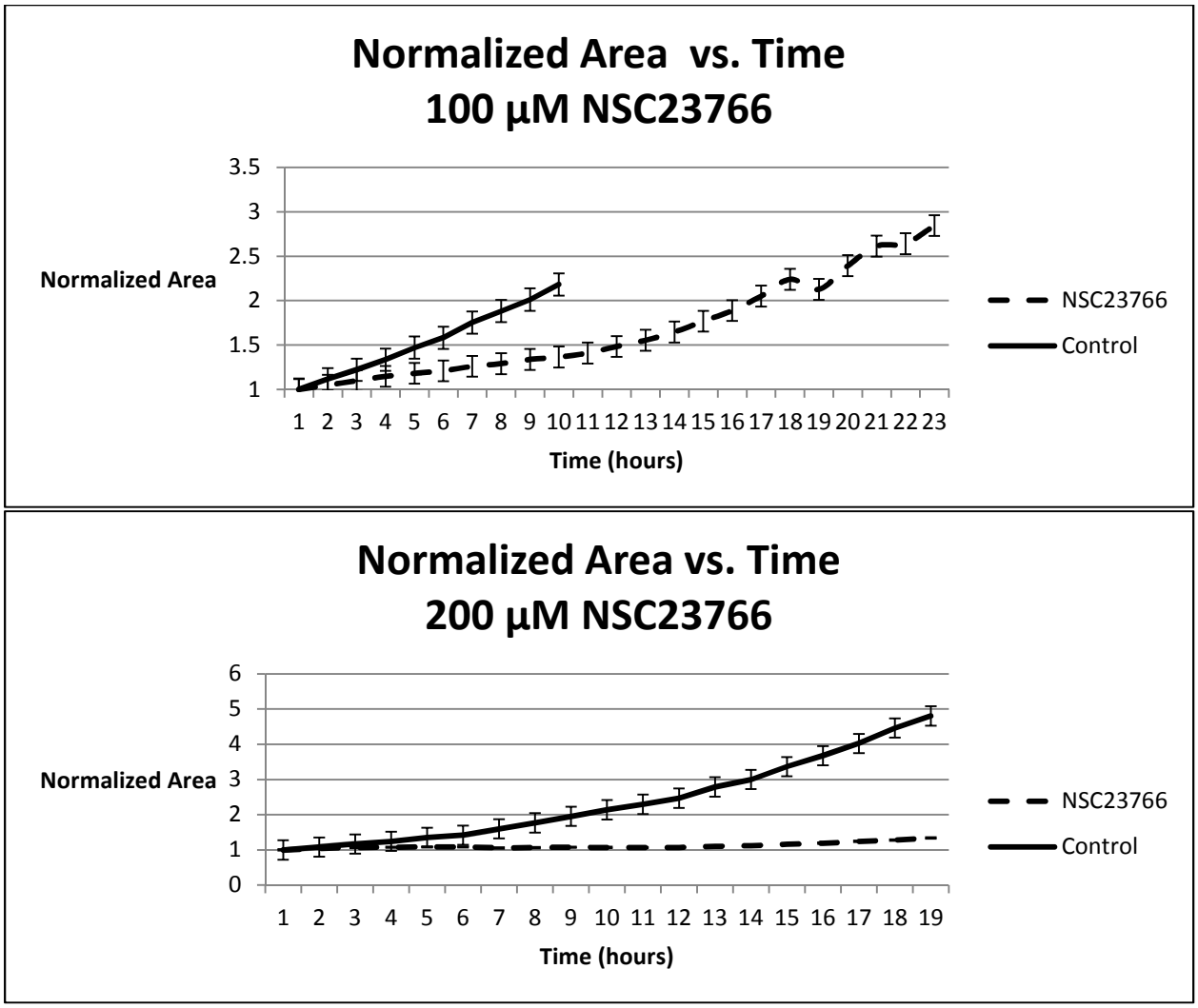

Figure 22: Area change of 100 µM and 200 µM NSC23766 (Rac1 Inhibitor). Each area was normalized to the first time point; standard error bars are shown for each time point. N = 4 for each control; N = 7 for 100 µM NSC23766; N = 8 for 200 µM NSC23766. Only 10 time points are shown for the 100 µM NSC23766 control because beyond 10 hours the edge of only 1 sample was still within the visually measureable area.

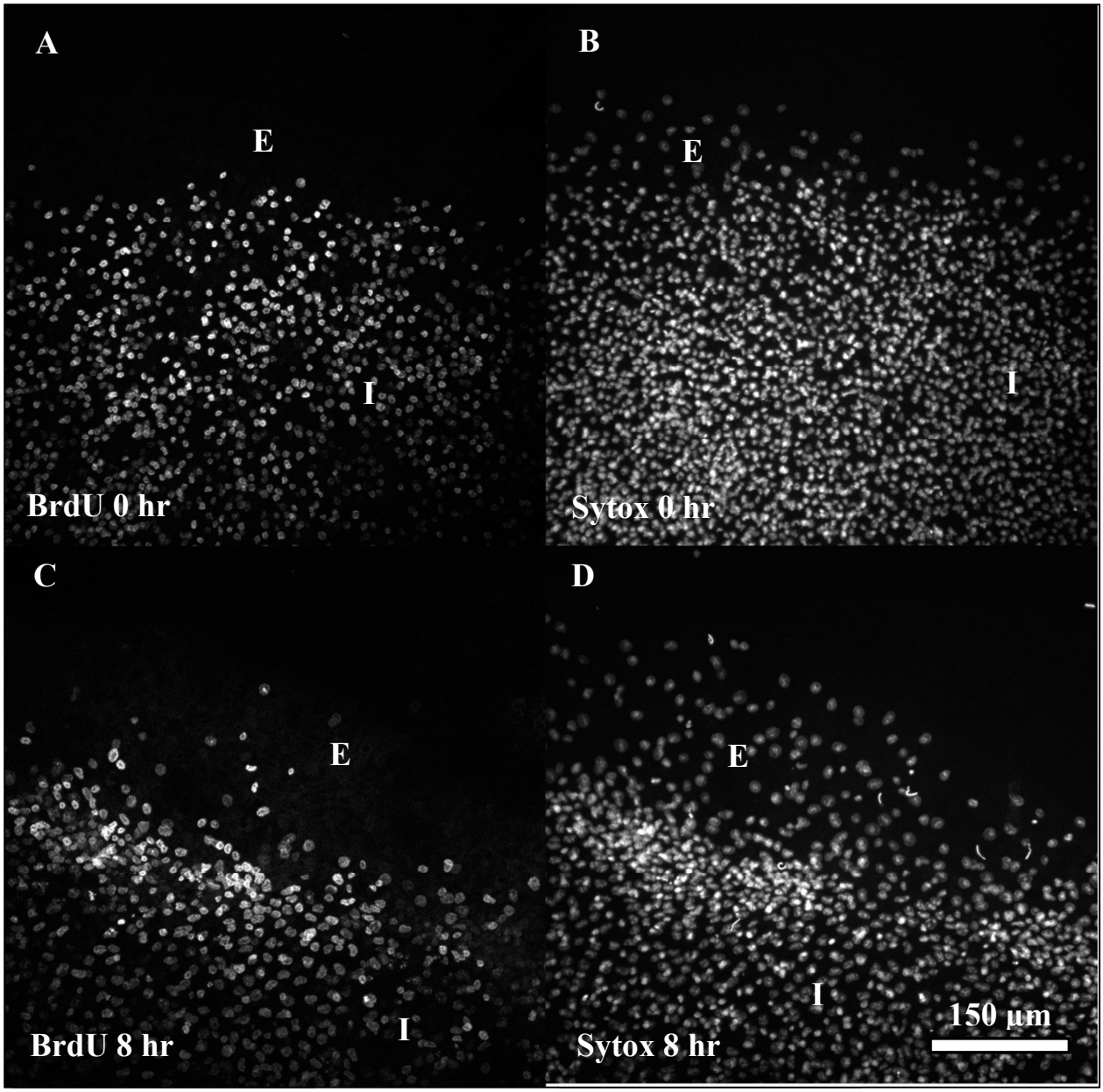

Figure 23: BrdU and Sytox treated embryos. The 0 hr treated embryos were fixed post-chase, while the 8 hr embryos were further incubated for 8 hrs post-chase and then fixed. "E" denotes the edge region, "I" denotes the interior zone.

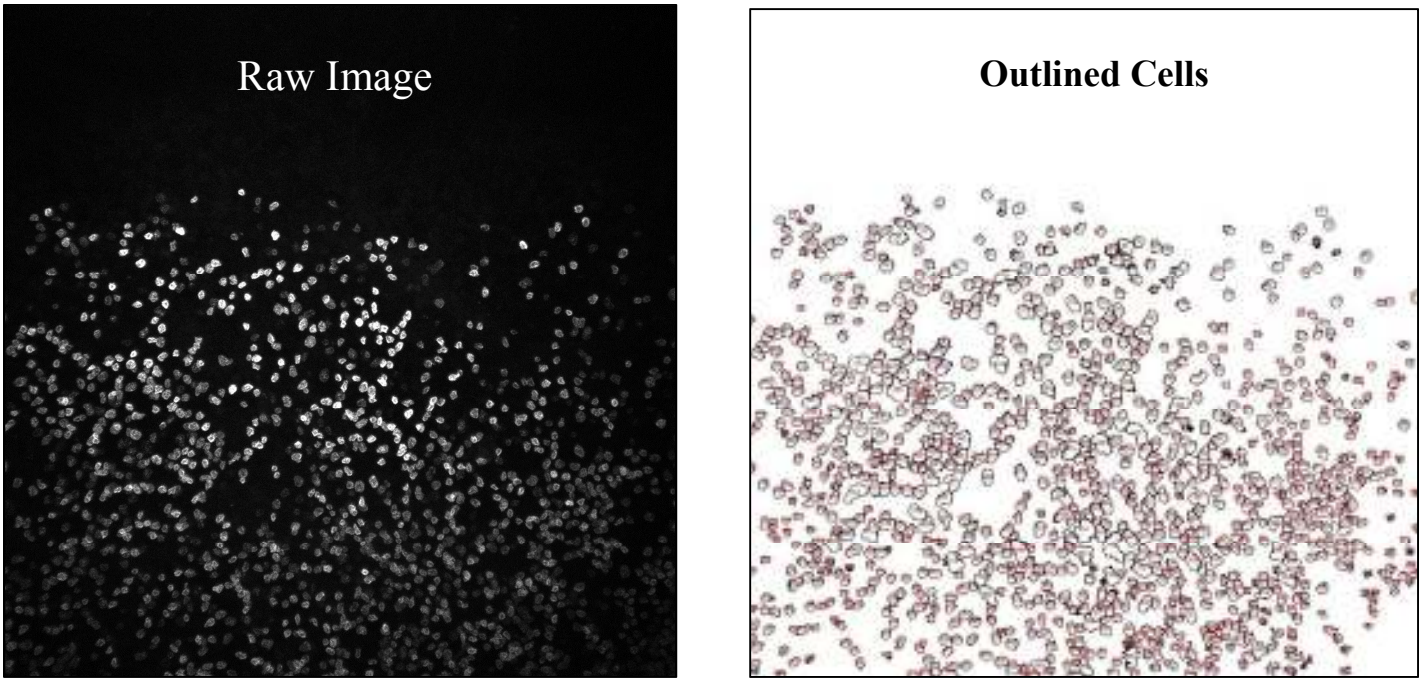

Figure 24: Representative images of pre-processed (Raw Image) and post-processed (Outlined Cells) cell outlines. Each outlined area is numbered (red regions within the outlines). The area fraction was calculated from the post-processed image.

	Sample	Area Fraction	
		BrdU	Sytox
0 hour	00	18.9	25.4
	01	32.8	33.3
	02	23.2	30.3
	03	27.1	41.1
	04	17.4	26
8 hour	05	16.1	23.8
	06	13.6	16.3
	07	16.3	19.5
	08	23.7	42.8
		Average Area	
		BrdU	Sytox
	0 hr	23.88	31.22
	8 hr	17.425	25.6

Table 1: Area fractions and average area fractions of BrdU and Sytox. The 0 hour time is for samples fixed immediately after a 4 hour room temperature chase; the 8 hour time is for samples incubated for 8 hours post-chase. Performing the Grubbs' Test for outliers showed that none were present.

REFERENCES

Ackland, M. L., D. F. Newgreen, et al. (2003). "Epidermal growth factor-induced epithelio-mesenchymal transition in human breast carcinoma cells." Lab Invest **83**(3): 435-448.

Adams, J. C. and M. A. Schwartz (2000). "Stimulation of fascin spikes by thrombospondin-1 is mediated by the GTPases Rac and Cdc42." J Cell Biol **150**(4): 807-822.

Arnoux, V., M. Nassour, et al. (2008). "Erk5 controls Slug expression and keratinocyte activation during wound healing." Mol Biol Cell **19**(11): 4738-4749.

Bachvarova, R. F., I. Skromne, et al. (1998). "Induction of primitive streak and Hensen's node by the posterior marginal zone in the early chick embryo." Development **125**(17): 3521-3534.

Ballestrem, C., B. Wehrle-Haller, et al. (1998). "Actin dynamics in living mammalian cells." J Cell Sci **111 (Pt 12)**: 1649-1658.

Bao, Z., Z. Zhao, et al. (2008). "Control of cell cycle timing during C. elegans embryogenesis." Dev Biol **318**(1): 65-72.

Bargagna-Mohan, P., A. Hamza, et al. (2007). "The tumor inhibitor and antiangiogenic agent withaferin A targets the intermediate filament protein vimentin." Chem Biol **14**(6): 623-634.

Bargagna-Mohan, P., R. R. Paranthan, et al. (2010). "Withaferin A targets intermediate filaments glial fibrillary acidic protein and vimentin in a model of retinal gliosis." J Biol Chem **285**(10): 7657-7669.

Bellairs, R. (1986). "The primitive streak." Anat Embryol (Berl) **174**(1): 1-14.

Bellairs, R., D. R. Bromham, et al. (1967). "The influence of the area opaca on the development of the young chick embryo." J Embryol Exp Morphol **17**(1): 195-212.

Bellairs, R., G. W. Ireland, et al. (1981). "The behaviour of embryonic chick and quail tissues in culture." J Embryol Exp Morphol **61**: 15-33.

Bortier, H., G. De Bruyne, et al. (1989). "Immunohistochemistry of laminin in early chicken and quail blastoderms." Anat Embryol (Berl) **180**(1): 65-69.

Brock, J., K. Midwinter, et al. (1996). "Healing of incisional wounds in the embryonic chick wing bud: characterization of the actin purse-string and demonstration of a requirement for Rho activation." J Cell Biol **135**(4): 1097-1107.

Cannito, S., E. Novo, et al. (2010). "Epithelial-mesenchymal transition: from molecular mechanisms, redox regulation to implications in human health and disease." Antioxid Redox Signal **12**(12): 1383-1430.

Cerda, J., M. Conrad, et al. (1998). "Zebrafish vimentin: molecular characterization, assembly properties and developmental expression." Eur J Cell Biol **77**(3): 175-187.

Chaffer, C. L., J. P. Brennan, et al. (2006). "Mesenchymal-to-epithelial transition facilitates bladder cancer metastasis: role of fibroblast growth factor receptor-2." Cancer Res **66**(23): 11271-11278.

Chapman, S. C., J. Collignon, et al. (2001). "Improved method for chick whole-embryo culture using a filter paper carrier." Dev Dyn **220**(3): 284-289.

Chernoff, E. A. (1989). "Adhesion and fusion of the extraembryonic epiblast." Tissue Cell **21**(5): 735-746.

Chou, Y. H., F. W. Flitney, et al. (2007). "The motility and dynamic properties of intermediate filaments and their constituent proteins." Exp Cell Res **313**(10): 2236-2243.

Christiansen, J. J. and A. K. Rajasekaran (2006). "Reassessing epithelial to mesenchymal transition as a prerequisite for carcinoma invasion and metastasis." Cancer Res **66**(17): 8319-8326.
Christofori, G. (2003). "Changing neighbours, changing behaviour: cell adhesion molecule-mediated signalling during tumour progression." EMBO J **22**(10): 2318-2323.
Ciesielski-Treska, J., G. Ulrich, et al. (1995). "Immunocytochemical localization of protein kinases Yes and Src in amoeboid microglia in culture: association of Yes kinase with vimentin intermediate filaments." Eur J Cell Biol **68**(4): 369-376.
Clarke, E. J. and V. Allan (2002). "Intermediate filaments: vimentin moves in." Curr Biol **12**(17): R596-598.
Critchley, D. R., M. A. England, et al. (1979). "Distribution of fibronectin in the ectoderm of gastrulating chick embryos." Nature **280**(5722): 498-500.
Danjo, Y. and I. K. Gipson (1998). "Actin 'purse string' filaments are anchored by E-cadherin-mediated adherens junctions at the leading edge of the epithelial wound, providing coordinated cell movement." J Cell Sci **111 (Pt 22)**: 3323-3332.
Davidson, L. A., B. G. Hoffstrom, et al. (2002). "Mesendoderm extension and mantle closure in Xenopus laevis gastrulation: combined roles for integrin alpha(5)beta(1), fibronectin, and tissue geometry." Dev Biol **242**(2): 109-129.
Dent, J. A., A. G. Polson, et al. (1989). "A whole-mount immunocytochemical analysis of the expression of the intermediate filament protein vimentin in Xenopus." Development **105**(1): 61-74.
DePianto, D. and P. A. Coulombe (2004). "Intermediate filaments and tissue repair." Exp Cell Res **301**(1): 68-76.
Downie, J. R. (1976). "The mechanism of chick blastoderm expansion." J Embryol Exp Morphol **35**(3): 559-575.
Downie, J. R. and S. M. Pegrum (1971). "Organization of the chick blastoderm edge." J Embryol Exp Morphol **26**(3): 623-635.
du Roure, O., A. Saez, et al. (2005). "Force mapping in epithelial cell migration." Proc Natl Acad Sci U S A **102**(7): 2390-2395.
Dulbecco, R., R. Allen, et al. (1983). "Functional changes of intermediate filaments in fibroblastic cells revealed by a monoclonal antibody." Proc Natl Acad Sci U S A **80**(7): 1915-1918.
Erickson, C. A., R. P. Tucker, et al. (1987). "Changes in the distribution of intermediate-filament types in Japanese quail embryos during morphogenesis." Differentiation **34**(2): 88-97.
Farooqui, R. and G. Fenteany (2005). "Multiple rows of cells behind an epithelial wound edge extend cryptic lamellipodia to collectively drive cell-sheet movement." J Cell Sci **118**(Pt 1): 51-63.
Fink, R. D. and M. S. Cooper (1996). "Apical membrane turnover is accelerated near cell-cell contacts in an embryonic epithelium." Dev Biol **174**(2): 180-189.
Fonck, E., G. G. Feigl, et al. (2009). "Effect of aging on elastin functionality in human cerebral arteries." Stroke **40**(7): 2552-2556.
Friedl, P. (2004). "Prespecification and plasticity: shifting mechanisms of cell migration." Curr Opin Cell Biol **16**(1): 14-23.
Friedl, P. and K. Wolf (2010). "Plasticity of cell migration: a multiscale tuning model." J Cell Biol **188**(1): 11-19.

Fuchs, E. and D. W. Cleveland (1998). "A structural scaffolding of intermediate filaments in health and disease." Science **279**(5350): 514-519.
Gallicano, G. I., P. Kouklis, et al. (1998). "Desmoplakin is required early in development for assembly of desmosomes and cytoskeletal linkage." J Cell Biol **143**(7): 2009-2022.
Garrod, D. R., A. J. Merritt, et al. (2002). "Desmosomal cadherins." Curr Opin Cell Biol **14**(5): 537-545.
Ghysen, A. and C. Dambly-Chaudiere (2004). "Development of the zebrafish lateral line." Curr Opin Neurobiol **14**(1): 67-73.
Gilles, C., M. Polette, et al. (1999). "Vimentin contributes to human mammary epithelial cell migration." J Cell Sci **112 (Pt 24)**: 4615-4625.
Goldman, R. D., S. Khuon, et al. (1996). "The function of intermediate filaments in cell shape and cytoskeletal integrity." J Cell Biol **134**(4): 971-983.
Goto, H., H. Kosako, et al. (1998). "Phosphorylation of vimentin by Rho-associated kinase at a unique amino-terminal site that is specifically phosphorylated during cytokinesis." J Biol Chem **273**(19): 11728-11736.
Goto, H., K. Tanabe, et al. (2002). "Phosphorylation and reorganization of vimentin by p21-activated kinase (PAK)." Genes Cells **7**(2): 91-97.
Gov, N. S. (2007). "Collective cell migration patterns: follow the leader." Proc Natl Acad Sci U S A **104**(41): 15970-15971.
Green, K. J. and C. A. Gaudry (2000). "Are desmosomes more than tethers for intermediate filaments?" Nat Rev Mol Cell Biol **1**(3): 208-216.
Green, K. J. and J. C. Jones (1996). "Desmosomes and hemidesmosomes: structure and function of molecular components." FASEB J **10**(8): 871-881.
Guzman, C., S. Jeney, et al. (2006). "Exploring the mechanical properties of single vimentin intermediate filaments by atomic force microscopy." J Mol Biol **360**(3): 623-630.
Gyoeva, F. K. and V. I. Gelfand (1991). "Coalignment of vimentin intermediate filaments with microtubules depends on kinesin." Nature **353**(6343): 445-448.
Hall, A. (1998). "Rho GTPases and the actin cytoskeleton." Science **279**(5350): 509-514.
Hamburger, V. and H. Hamilton (1951). "A series of normal stages in the development of the chick embryo." Journal of Morphology **88**(1).
Hammerle, B. and F. J. Tejedor (2002). "A method for pulse and chase BrdU-labeling of early chick embryos." J Neurosci Methods **122**(1): 59-64.
Herrmann, H., H. Bar, et al. (2007). "Intermediate filaments: from cell architecture to nanomechanics." Nat Rev Mol Cell Biol **8**(7): 562-573.
Herrmann, H., B. Fouquet, et al. (1989). "Expression of intermediate filament proteins during development of Xenopus laevis. I. cDNA clones encoding different forms of vimentin." Development **105**(2): 279-298.
Huber, A. H., D. B. Stewart, et al. (2001). "The cadherin cytoplasmic domain is unstructured in the absence of beta-catenin. A possible mechanism for regulating cadherin turnover." J Biol Chem **276**(15): 12301-12309.
Ihara, S. and Y. Motobayashi (1992). "Wound closure in foetal rat skin." Development **114**(3): 573-582.
Inagaki, M., Y. Nishi, et al. (1987). "Site-specific phosphorylation induces disassembly of vimentin filaments in vitro." Nature **328**(6131): 649-652.
Ingber, D. E. (2006). "Mechanical control of tissue morphogenesis during embryological development." Int J Dev Biol **50**(2-3): 255-266.

Jacinto, A., A. Martinez-Arias, et al. (2001). "Mechanisms of epithelial fusion and repair." Nat Cell Biol **3**(5): E117-123.
Jacinto, A., W. Wood, et al. (2002). "Dynamic analysis of actin cable function during Drosophila dorsal closure." Curr Biol **12**(14): 1245-1250.
Janmey, P. A., J. V. Shah, et al. (1998). "Viscoelasticity of intermediate filament networks." Subcell Biochem **31**: 381-397.
Janosch, P., A. Kieser, et al. (2000). "The Raf-1 kinase associates with vimentin kinases and regulates the structure of vimentin filaments." FASEB J **14**(13): 2008-2021.
Jou, T. S., D. B. Stewart, et al. (1995). "Genetic and biochemical dissection of protein linkages in the cadherin-catenin complex." Proc Natl Acad Sci U S A **92**(11): 5067-5071.
Kaileh, M., W. Vanden Berghe, et al. (2007). "Withaferin a strongly elicits IkappaB kinase beta hyperphosphorylation concomitant with potent inhibition of its kinase activity." J Biol Chem **282**(7): 4253-4264.
Keller, R. (2005). "Cell migration during gastrulation." Curr Opin Cell Biol **17**(5): 533-541.
Keller, R., L. A. Davidson, et al. (2003). "How we are shaped: the biomechanics of gastrulation." Differentiation **71**(3): 171-205.
Keller, R. E. (1980). "The cellular basis of epiboly: an SEM study of deep-cell rearrangement during gastrulation in Xenopus laevis." J Embryol Exp Morphol **60**: 201-234.
Kiehart, D. P., C. G. Galbraith, et al. (2000). "Multiple forces contribute to cell sheet morphogenesis for dorsal closure in Drosophila." J Cell Biol **149**(2): 471-490.
Kokkinos, M. I., R. Wafai, et al. (2007). "Vimentin and epithelial-mesenchymal transition in human breast cancer--observations in vitro and in vivo." Cells Tissues Organs **185**(1-3): 191-203.
Kolega, J. (1986). "Effects of mechanical tension on protrusive activity and microfilament and intermediate filament organization in an epidermal epithelium moving in culture." J Cell Biol **102**(4): 1400-1411.
Koppen, M., B. G. Fernandez, et al. (2006). "Coordinated cell-shape changes control epithelial movement in zebrafish and Drosophila." Development **133**(14): 2671-2681.
Lahat, G., Q. S. Zhu, et al. (2010). "Vimentin is a novel anti-cancer therapeutic target; insights from in vitro and in vivo mice xenograft studies." PLoS One **5**(4): e10105.
Lash, J. W., E. Gosfield, 3rd, et al. (1990). "Migration of chick blastoderm under the vitelline membrane: the role of fibronectin." Dev Biol **139**(2): 407-416.
Ledent, V. (2002). "Postembryonic development of the posterior lateral line in zebrafish." Development **129**(3): 597-604.
Lee, J. M., S. Dedhar, et al. (2006). "The epithelial-mesenchymal transition: new insights in signaling, development, and disease." J Cell Biol **172**(7): 973-981.
Lequarre, A. S., J. Marchandise, et al. (2003). "Cell cycle duration at the time of maternal zygotic transition for in vitro produced bovine embryos: effect of oxygen tension and transcription inhibition." Biol Reprod **69**(5): 1707-1713.
Madlener, M., C. Mauch, et al. (1996). "Regulation of the expression of stromelysin-2 by growth factors in keratinocytes: implications for normal and impaired wound healing." Biochem J **320 (Pt 2)**: 659-664.
Magin, T. M., P. Vijayaraj, et al. (2007). "Structural and regulatory functions of keratins." Exp Cell Res **313**(10): 2021-2032.

Mandato, C. A. and W. M. Bement (2001). "Contraction and polymerization cooperate to assemble and close actomyosin rings around Xenopus oocyte wounds." J Cell Biol **154**(4): 785-797.
Martin, P. and J. Lewis (1992). "Actin cables and epidermal movement in embryonic wound healing." Nature **360**(6400): 179-183.
Meriane, M., S. Mary, et al. (2000). "Cdc42Hs and Rac1 GTPases induce the collapse of the vimentin intermediate filament network." J Biol Chem **275**(42): 33046-33052.
Moll, J., G. Sansig, et al. (1991). "The murine rac1 gene: cDNA cloning, tissue distribution and regulated expression of rac1 mRNA by disassembly of actin microfilaments." Oncogene **6**(5): 863-866.
Mucke, N., L. Kreplak, et al. (2004). "Assessing the flexibility of intermediate filaments by atomic force microscopy." J Mol Biol **335**(5): 1241-1250.
New, D. A. (1959). "The adhesive properties and expansion of the chick blastoderm." J Embryol Exp Morphol **7**: 146-164.
Olivier, N., M. A. Luengo-Oroz, et al. (2010). "Cell lineage reconstruction of early zebrafish embryos using label-free nonlinear microscopy." Science **329**(5994): 967-971.
Omelchenko, T., J. M. Vasiliev, et al. (2003). "Rho-dependent formation of epithelial "leader" cells during wound healing." Proc Natl Acad Sci U S A **100**(19): 10788-10793.
Page, M. (1989). "Changing patterns of cytokeratins and vimentin in the early chick embryo." Development **105**(1): 97-107.
Polette, M., M. Mestdagt, et al. (2007). "Beta-catenin and ZO-1: shuttle molecules involved in tumor invasion-associated epithelial-mesenchymal transition processes." Cells Tissues Organs **185**(1-3): 61-65.
Poujade, M., E. Grasland-Mongrain, et al. (2007). "Collective migration of an epithelial monolayer in response to a model wound." Proc Natl Acad Sci U S A **104**(41): 15988-15993.
Prahlad, V., M. Yoon, et al. (1998). "Rapid movements of vimentin on microtubule tracks: kinesin-dependent assembly of intermediate filament networks." J Cell Biol **143**(1): 159-170.
Raddatz, E., F. Monnet-Tschudi, et al. (1991). "Fibronectin distribution in the chick embryo during formation of the blastula." Anat Embryol (Berl) **183**(1): 57-65.
Rechardt, O., O. Elomaa, et al. (2000). "Stromelysin-2 is upregulated during normal wound repair and is induced by cytokines." J Invest Dermatol **115**(5): 778-787.
Revenu, C. and D. Gilmour (2009). "EMT 2.0: shaping epithelia through collective migration." Curr Opin Genet Dev **19**(4): 338-342.
Ridley, A. (2000). "Rho GTPases. Integrating integrin signaling." J Cell Biol **150**(4): F107-109.
Ridley, A. J. (2001). "Rho GTPases and cell migration." J Cell Sci **114**(Pt 15): 2713-2722.
Ridley, A. J., M. A. Schwartz, et al. (2003). "Cell migration: integrating signals from front to back." Science **302**(5651): 1704-1709.
Roeser, T., S. Stein, et al. (1999). "Nuclear beta-catenin and the development of bilateral symmetry in normal and LiCl-exposed chick embryos." Development **126**(13): 2955-2965.
Salmela, M. T., S. L. Pender, et al. (2004). "Collagenase-1 (MMP-1), matrilysin-1 (MMP-7), and stromelysin-2 (MMP-10) are expressed by migrating enterocytes during intestinal wound healing." Scand J Gastroenterol **39**(11): 1095-1104.

Sanders, E. J., M. Varedi, et al. (1993). "Cell proliferation in the gastrulating chick embryo: a study using BrdU incorporation and PCNA localization." Development **118**(2): 389-399.
Shah, J. V., L. Z. Wang, et al. (1998). "Interaction of vimentin with actin and phospholipids." Biol Bull **194**(3): 402-405.
Srinivasan, S., R. S. Ranga, et al. (2007). "Par-4-dependent apoptosis by the dietary compound withaferin A in prostate cancer cells." Cancer Res **67**(1): 246-253.
Stern, C. D., S. E. Fraser, et al. (1988). "A cell lineage analysis of segmentation in the chick embryo." Development **104 Suppl**: 231-244.
Sugihara, K., N. Nakatsuji, et al. (1998). "Rac1 is required for the formation of three germ layers during gastrulation." Oncogene **17**(26): 3427-3433.
Takaishi, K., T. Sasaki, et al. (1997). "Regulation of cell-cell adhesion by rac and rho small G proteins in MDCK cells." J Cell Biol **139**(4): 1047-1059.
Tapon, N. and A. Hall (1997). "Rho, Rac and Cdc42 GTPases regulate the organization of the actin cytoskeleton." Curr Opin Cell Biol **9**(1): 86-92.
Toyama, Y., X. G. Peralta, et al. (2008). "Apoptotic force and tissue dynamics during Drosophila embryogenesis." Science **321**(5896): 1683-1686.
Trepat, X., M. R. Wasserman, et al. (2009). "Physical forces during collective cell migration." Nature Physics **5**.
Trinkhaus, J. P. (1984). Cells into Organs: The Forces that Shape the Embryo. Englewood Cliffs, NJ, Prentice Hall.
Valgeirsdottir, S., L. Claesson-Welsh, et al. (1998). "PDGF induces reorganization of vimentin filaments." J Cell Sci **111 (Pt 14)**: 1973-1980.
Van Aelst, L. and C. D'Souza-Schorey (1997). "Rho GTPases and signaling networks." Genes Dev **11**(18): 2295-2322.
Vasilyev, A., Y. Liu, et al. (2009). "Collective cell migration drives morphogenesis of the kidney nephron." PLoS Biol **7**(1): e9.
Wang, N. and D. Stamenovic (2002). "Mechanics of vimentin intermediate filaments." J Muscle Res Cell Motil **23**(5-6): 535-540.
Weliky, M. and G. Oster (1990). "The mechanical basis of cell rearrangement. I. Epithelial morphogenesis during Fundulus epiboly." Development **109**(2): 373-386.
Wenk, M. B., K. S. Midwood, et al. (2000). "Tenascin-C suppresses Rho activation." J Cell Biol **150**(4): 913-920.
Wood, A. and L. Timmermans (1988). "Teleost epiboly: a reassessment of deep cell movement in the germ ring." Development **102**: 575-585.
Yang, H., G. Shi, et al. (2007). "The tumor proteasome is a primary target for the natural anticancer compound Withaferin A isolated from "Indian winter cherry"." Mol Pharmacol **71**(2): 426-437.
Yoon, K. H., M. Yoon, et al. (2001). "Insights into the dynamic properties of keratin intermediate filaments in living epithelial cells." J Cell Biol **153**(3): 503-516.
Zalik, S. E., E. Lewandowski, et al. (1999). "Cell adhesion and the actin cytoskeleton of the enveloping layer in the zebrafish embryo during epiboly." Biochem Cell Biol **77**(6): 527-542.
Zamir, E. A., B. J. Rongish, et al. (2008). "The ECM moves during primitive streak formation--computation of ECM versus cellular motion." PLoS Biol **6**(10): e247.